Three Layer Fresnel Reflection Coefficents

Aaron Webster

February 16, 2012

0.1 Metal-BK7-Air

0.1.1 Ag-BK7-Vacuum

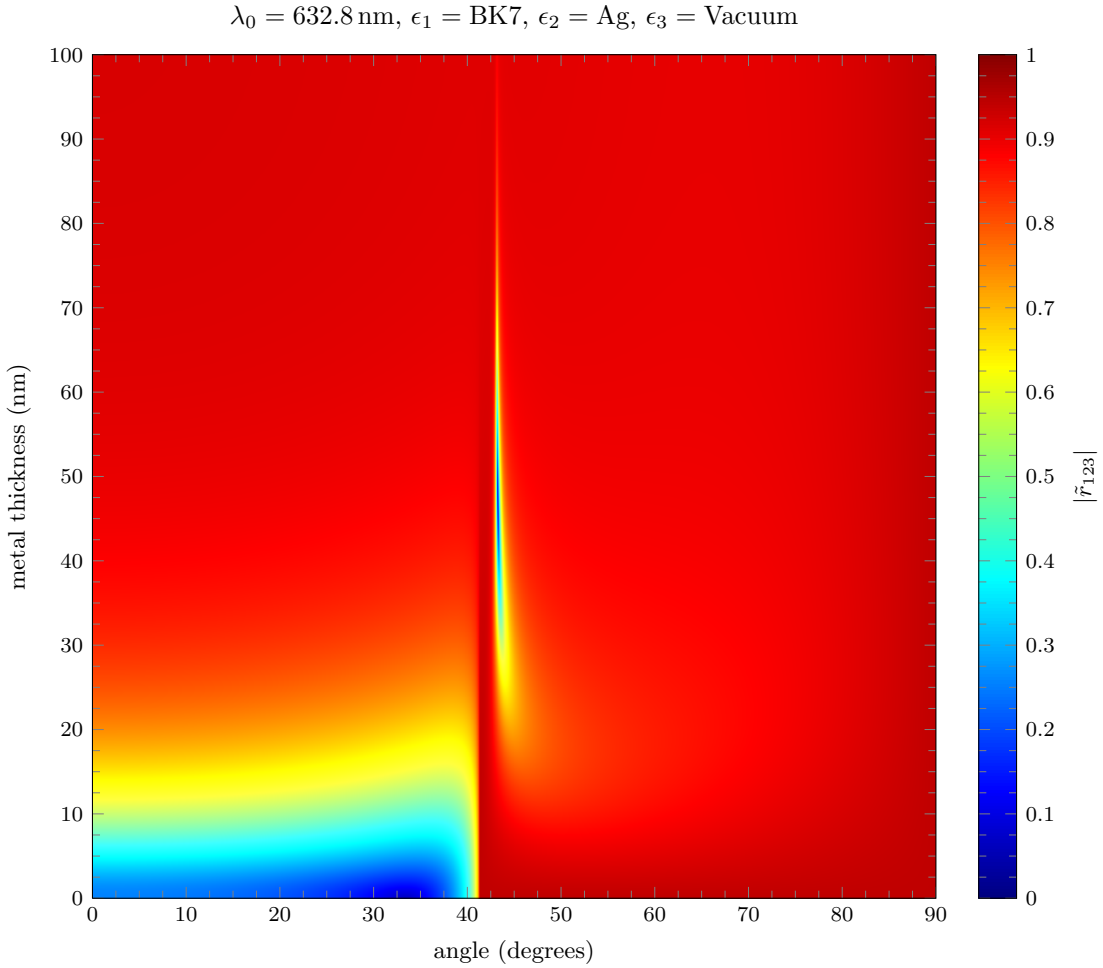

Figure 1: Reflection coefficent $|\tilde{r}_{123}|$ for the three layer fresnel system (Ag-BK7-Vacuum) as a function of incident angle and thickness of the metal layer ϵ_2. Numeric values of the permittivity are found in Table **??**

0.1.2 Al-BK7-Vacuum

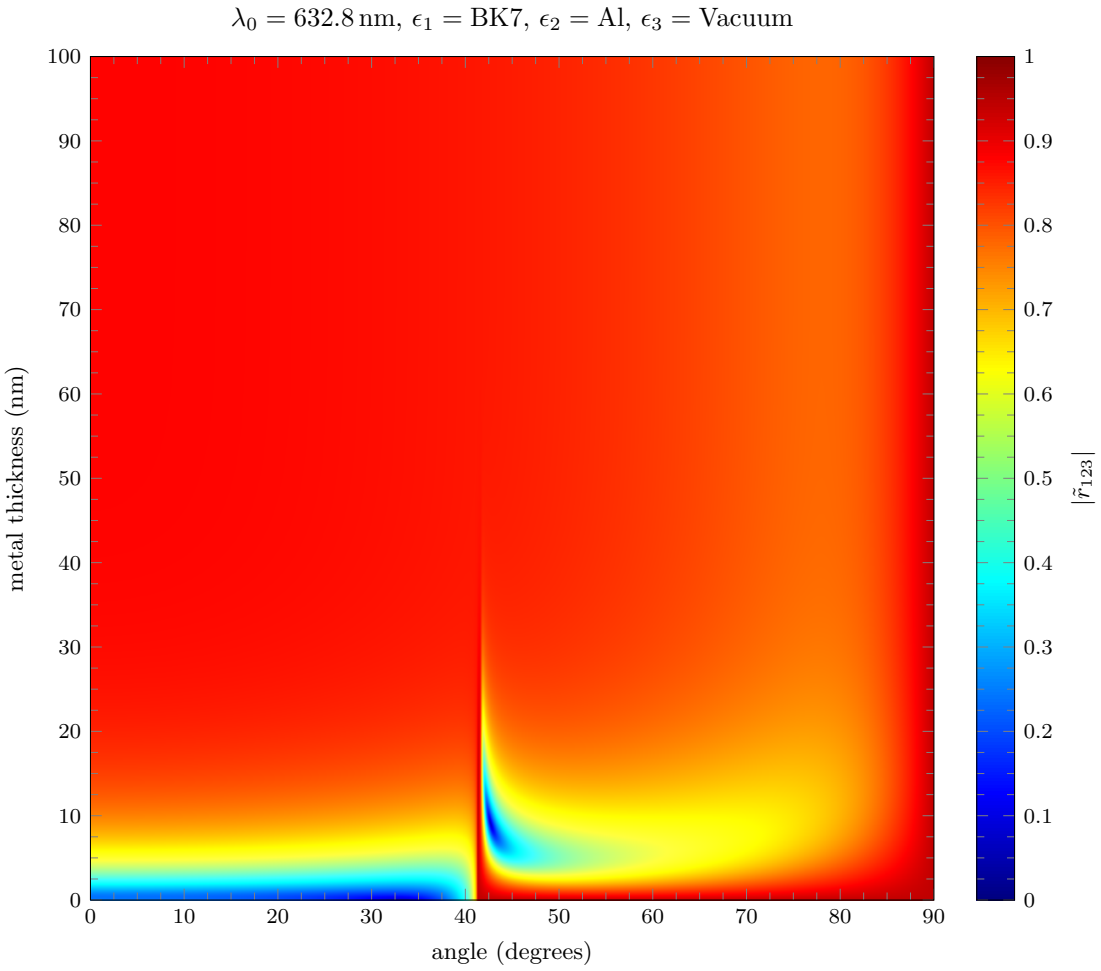

Figure 2: Reflection coefficent $|\tilde{r}_{123}|$ for the three layer fresnel system (Al-BK7-Vacuum) as a function of incident angle and thickness of the metal layer ϵ_2. Numeric values of the permittivity are found in Table **??**

0.1.3 Au-BK7-Vacuum

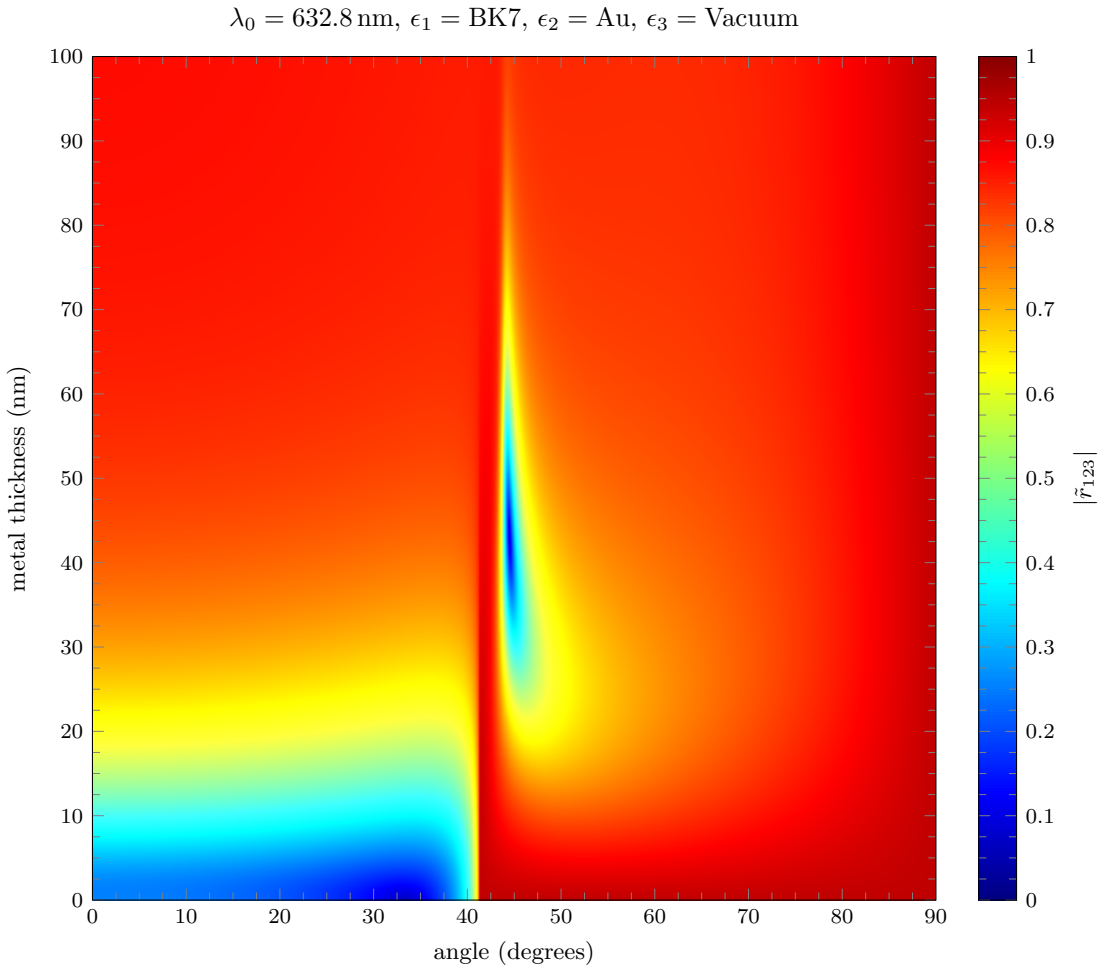

Figure 3: Reflection coefficent $|\tilde{r}_{123}|$ for the three layer fresnel system (Au-BK7-Vacuum) as a function of incident angle and thickness of the metal layer ϵ_2. Numeric values of the permittivity are found in Table **??**

0.1.4 Be-BK7-Vacuum

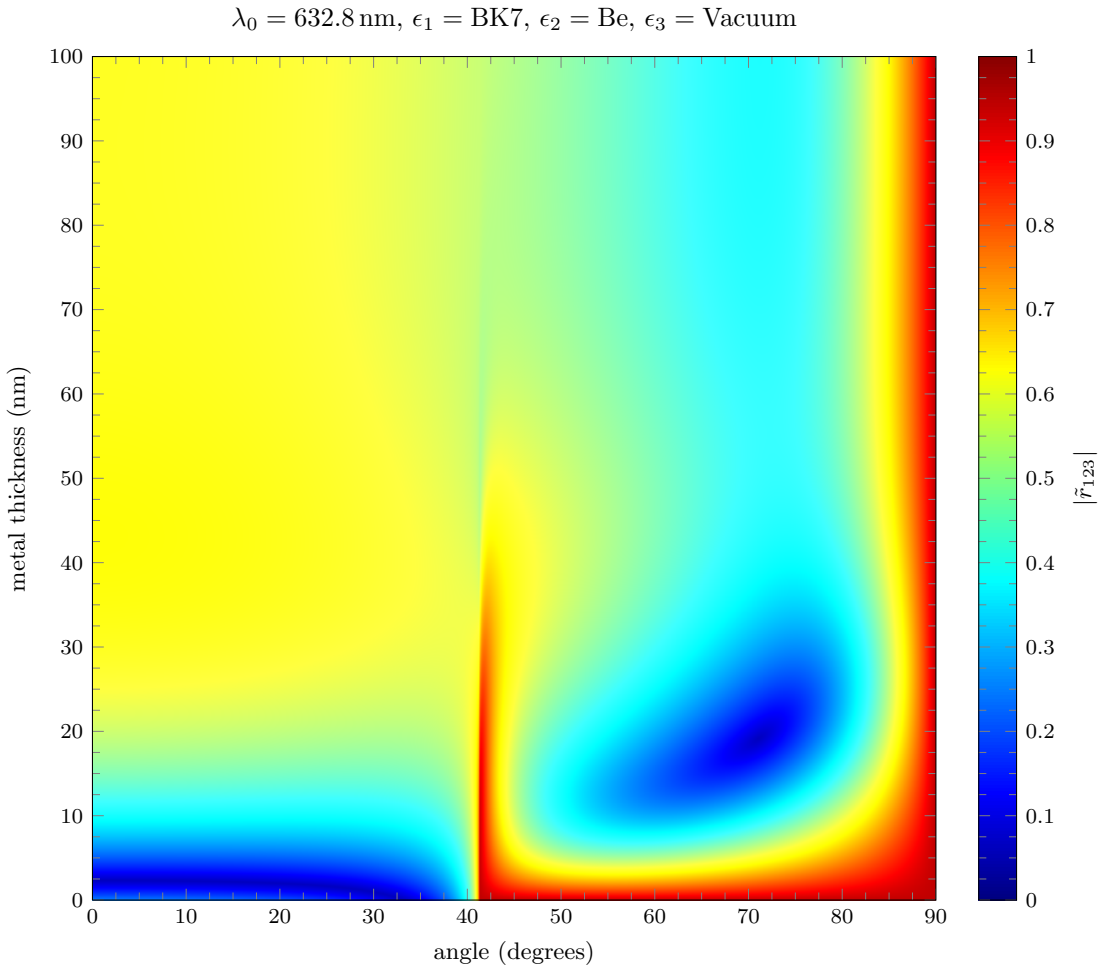

Figure 4: Reflection coefficent $|\tilde{r}_{123}|$ for the three layer fresnel system (Be-BK7-Vacuum) as a function of incident angle and thickness of the metal layer ϵ_2. Numeric values of the permittivity are found in Table **??**

0.1.5 Cr-BK7-Vacuum

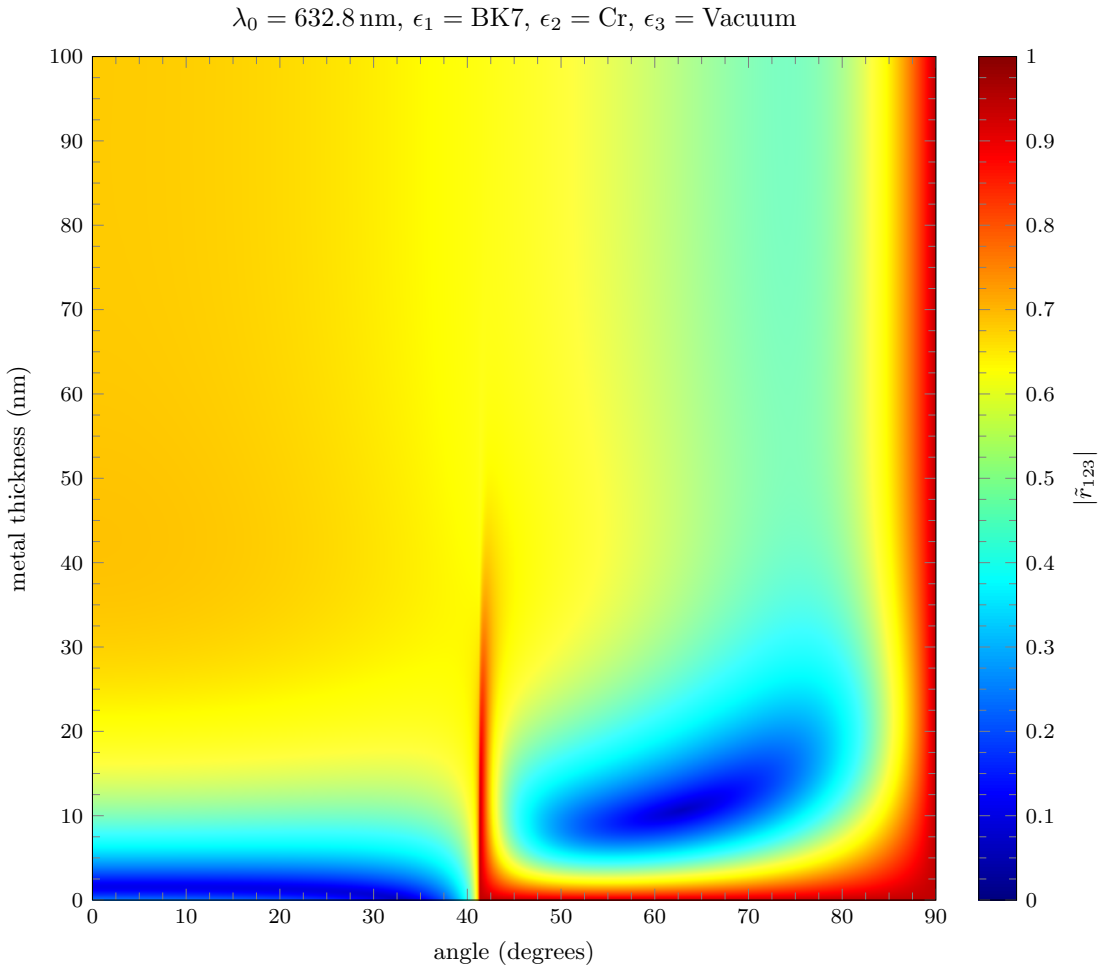

Figure 5: Reflection coefficent $|\tilde{r}_{123}|$ for the three layer fresnel system (Cr-BK7-Vacuum) as a function of incident angle and thickness of the metal layer ϵ_2. Numeric values of the permittivity are found in Table **??**

0.1.6 Cu-BK7-Vacuum

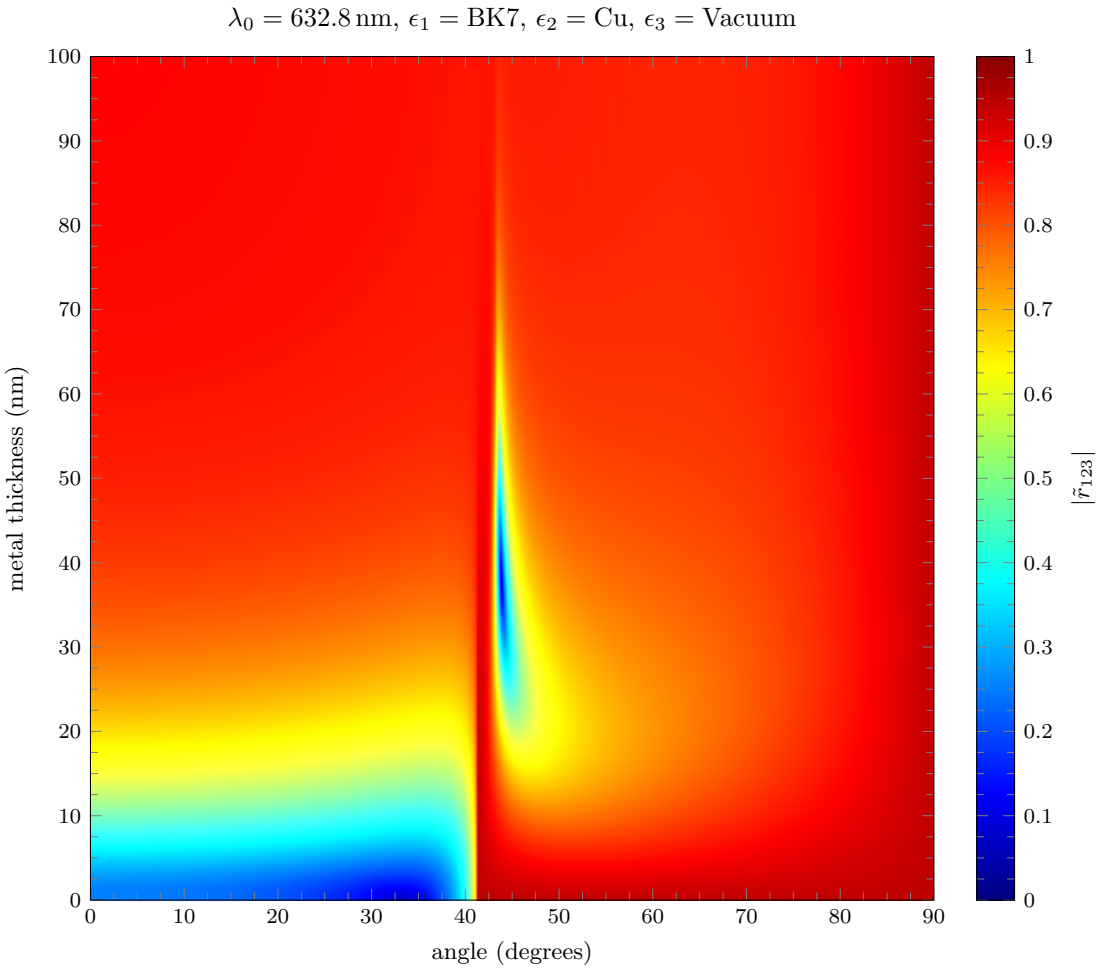

Figure 6: Reflection coefficent $|\tilde{r}_{123}|$ for the three layer fresnel system (Cu-BK7-Vacuum) as a function of incident angle and thickness of the metal layer ϵ_2. Numeric values of the permittivity are found in Table **??**

0.1.7 Ni-BK7-Vacuum

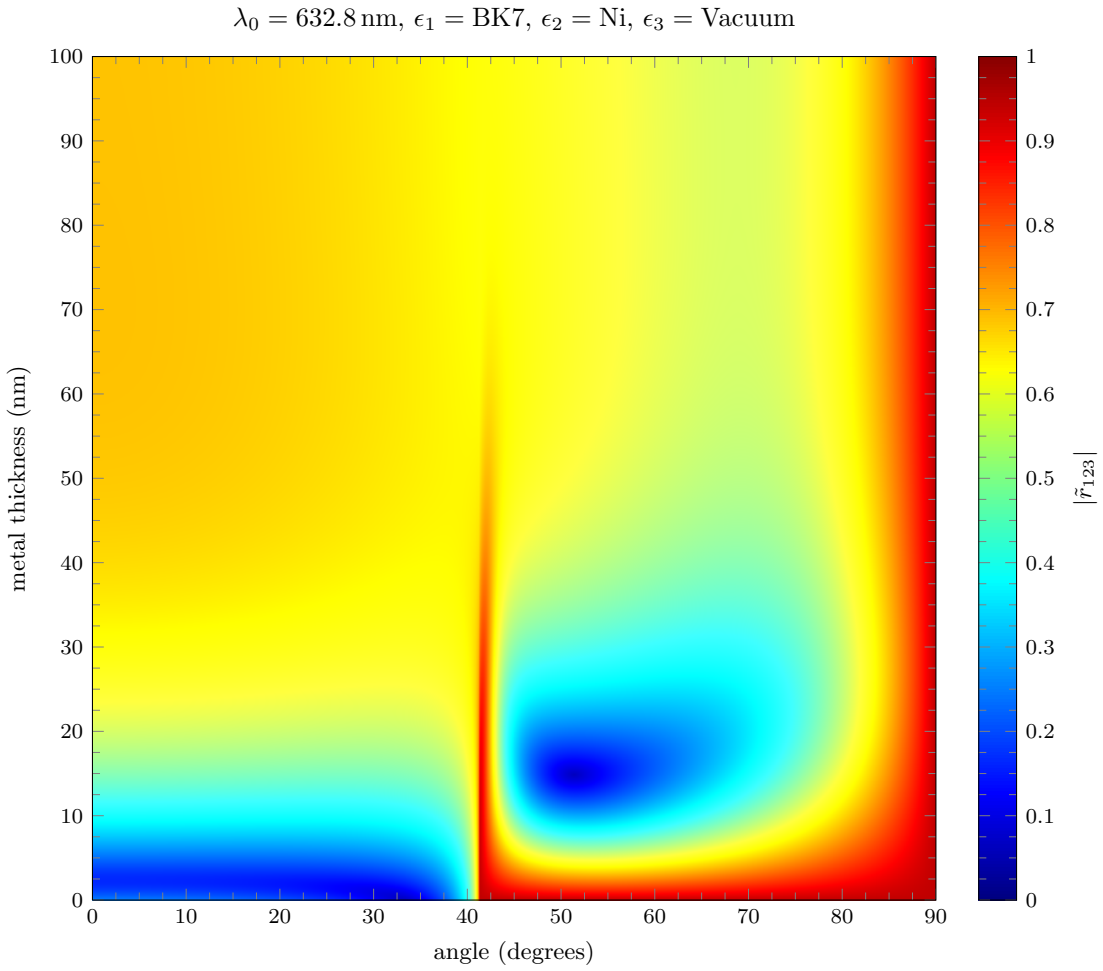

Figure 7: Reflection coefficent $|\tilde{r}_{123}|$ for the three layer fresnel system (Ni-BK7-Vacuum) as a function of incident angle and thickness of the metal layer ϵ_2. Numeric values of the permittivity are found in Table **??**

0.1.8 Pd-BK7-Vacuum

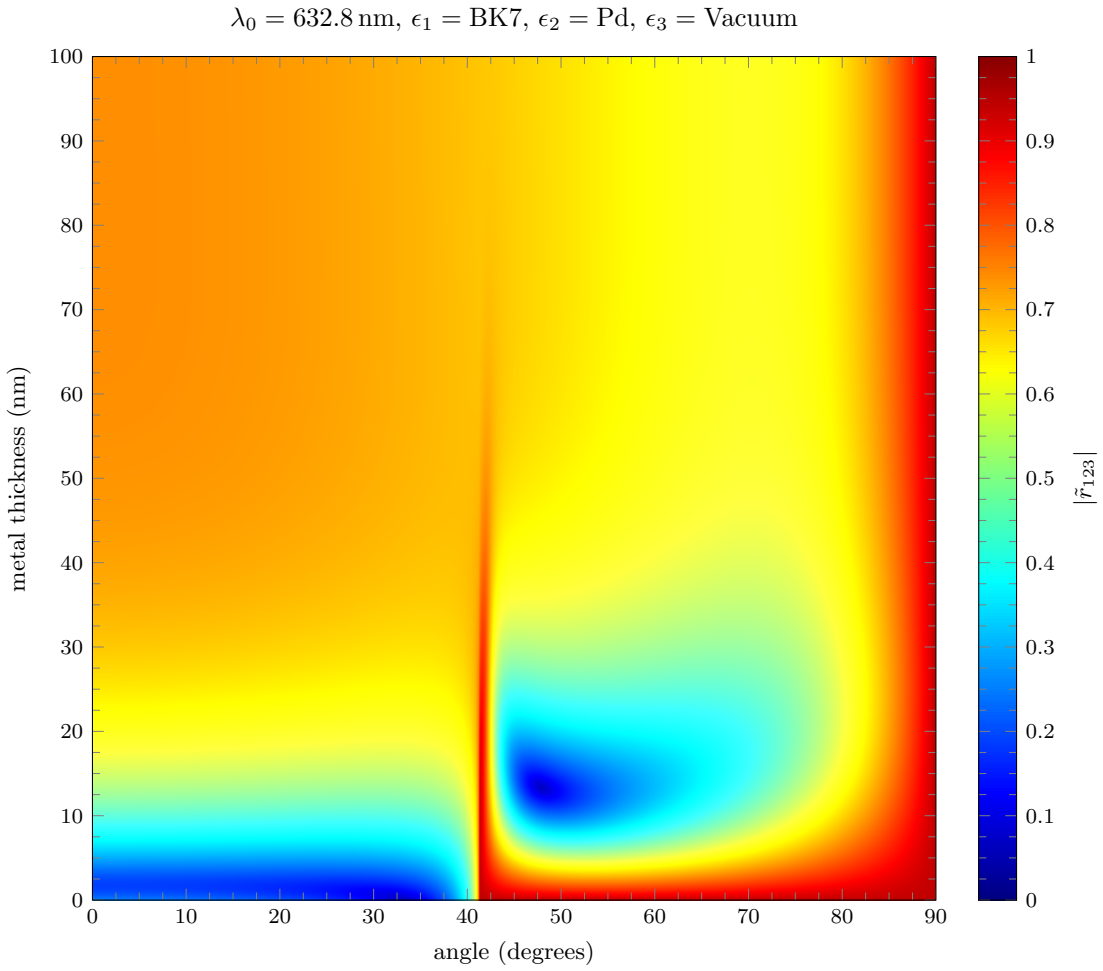

Figure 8: Reflection coefficent $|\tilde{r}_{123}|$ for the three layer fresnel system (Pd-BK7-Vacuum) as a function of incident angle and thickness of the metal layer ϵ_2. Numeric values of the permittivity are found in Table **??**

0.1.9 Pt-BK7-Vacuum

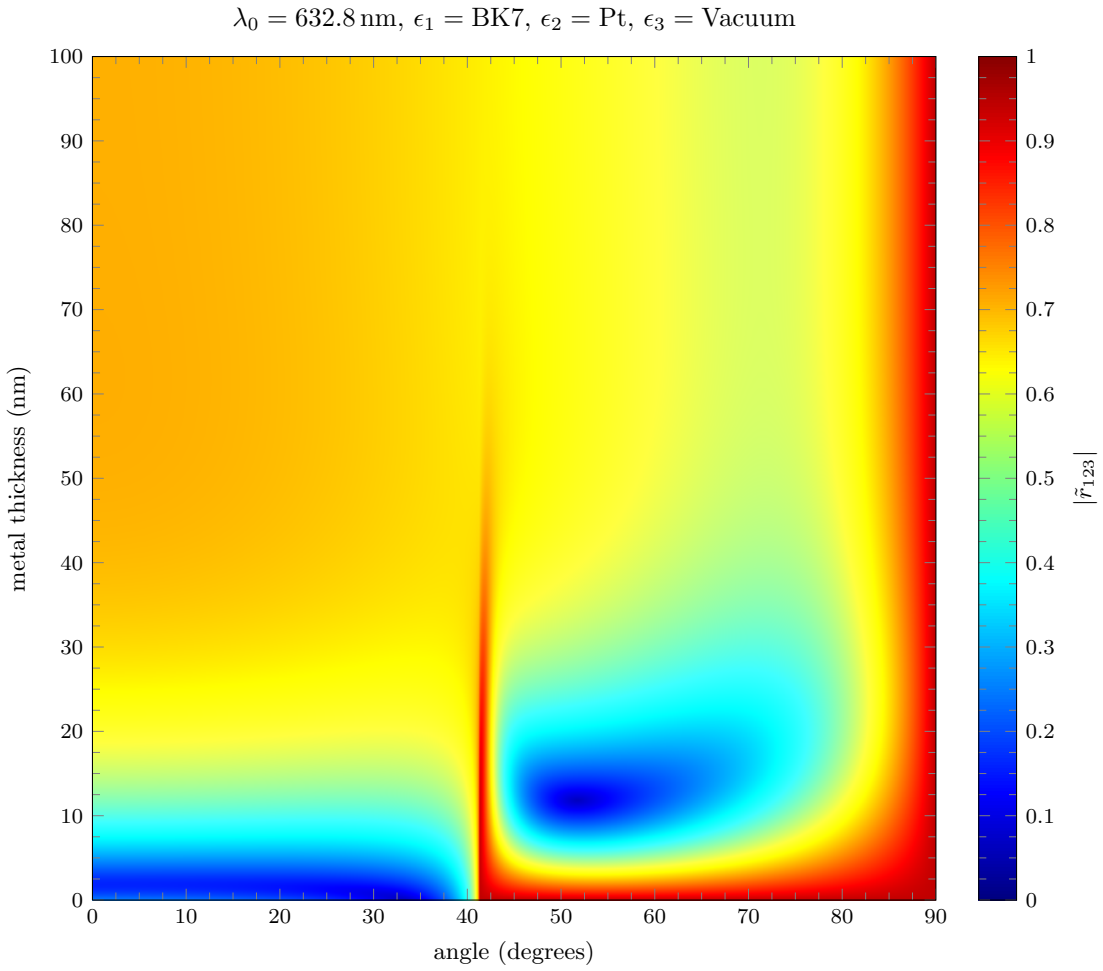

Figure 9: Reflection coefficent $|\tilde{r}_{123}|$ for the three layer fresnel system (Pt-BK7-Vacuum) as a function of incident angle and thickness of the metal layer ϵ_2. Numeric values of the permittivity are found in Table **??**

0.1.10 Ti-BK7-Vacuum

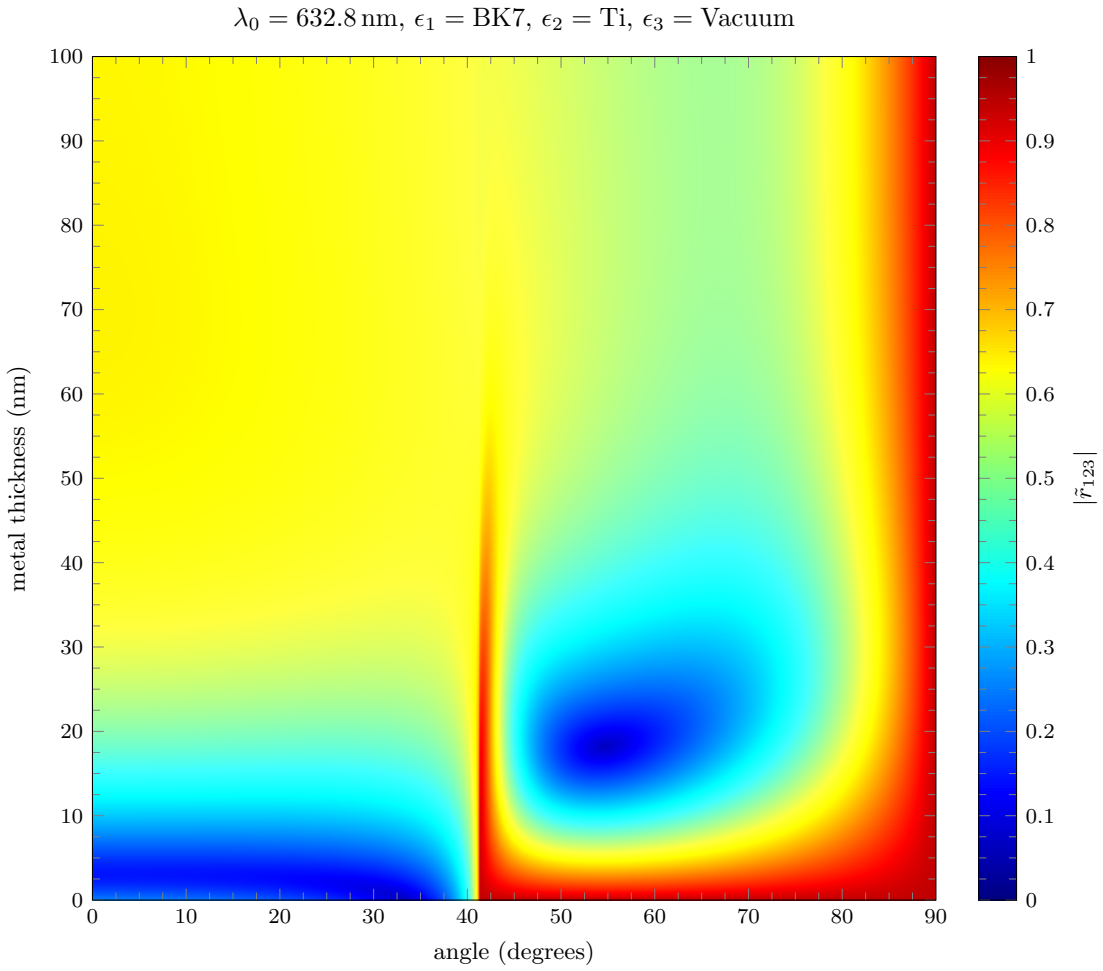

Figure 10: Reflection coefficent $|\tilde{r}_{123}|$ for the three layer fresnel system (Ti-BK7-Vacuum) as a function of incident angle and thickness of the metal layer ϵ_2. Numeric values of the permittivity are found in Table **??**

0.1.11 W-BK7-Vacuum

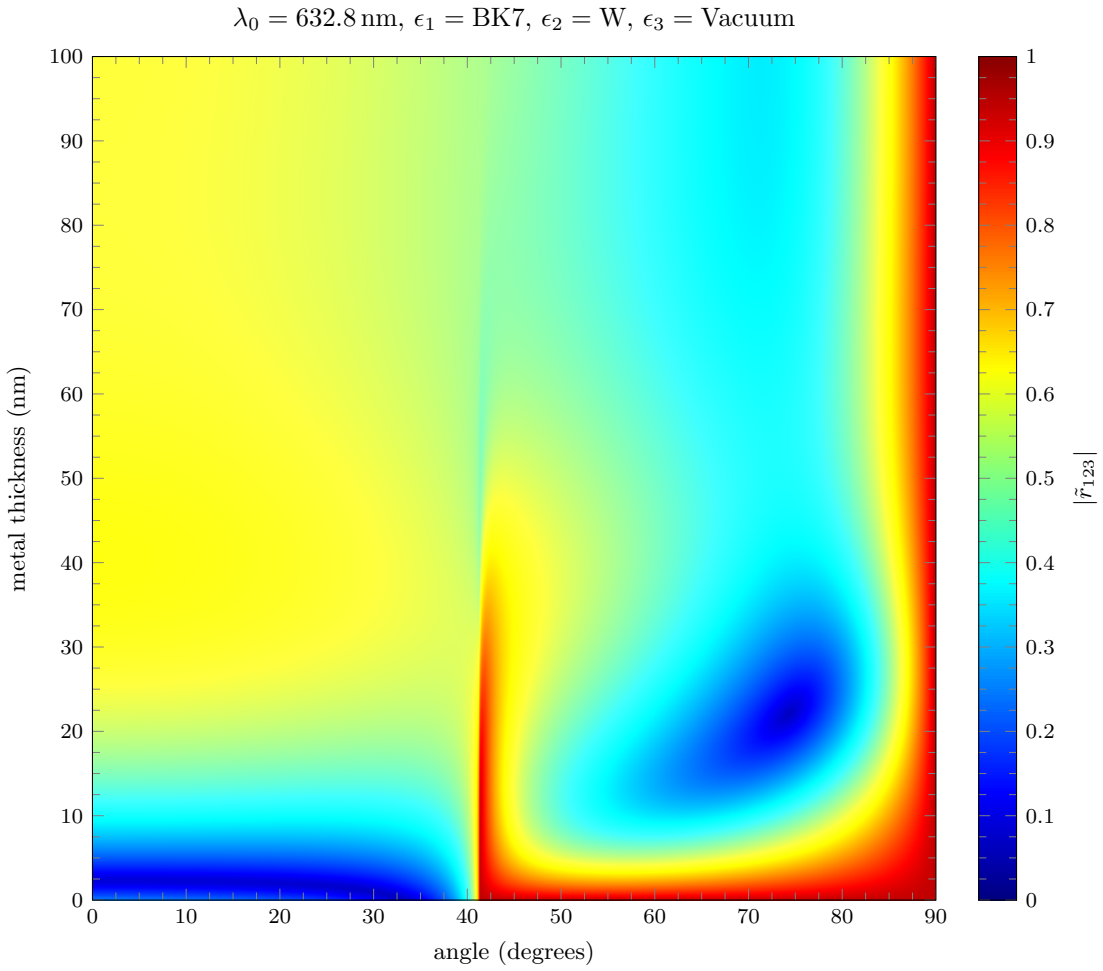

Figure 11: Reflection coefficent $|\tilde{r}_{123}|$ for the three layer fresnel system (W-BK7-Vacuum) as a function of incident angle and thickness of the metal layer ϵ_2. Numeric values of the permittivity are found in Table **??**

0.2 Metal-LAH79-Air

0.2.1 Ag-LAH79-Vacuum

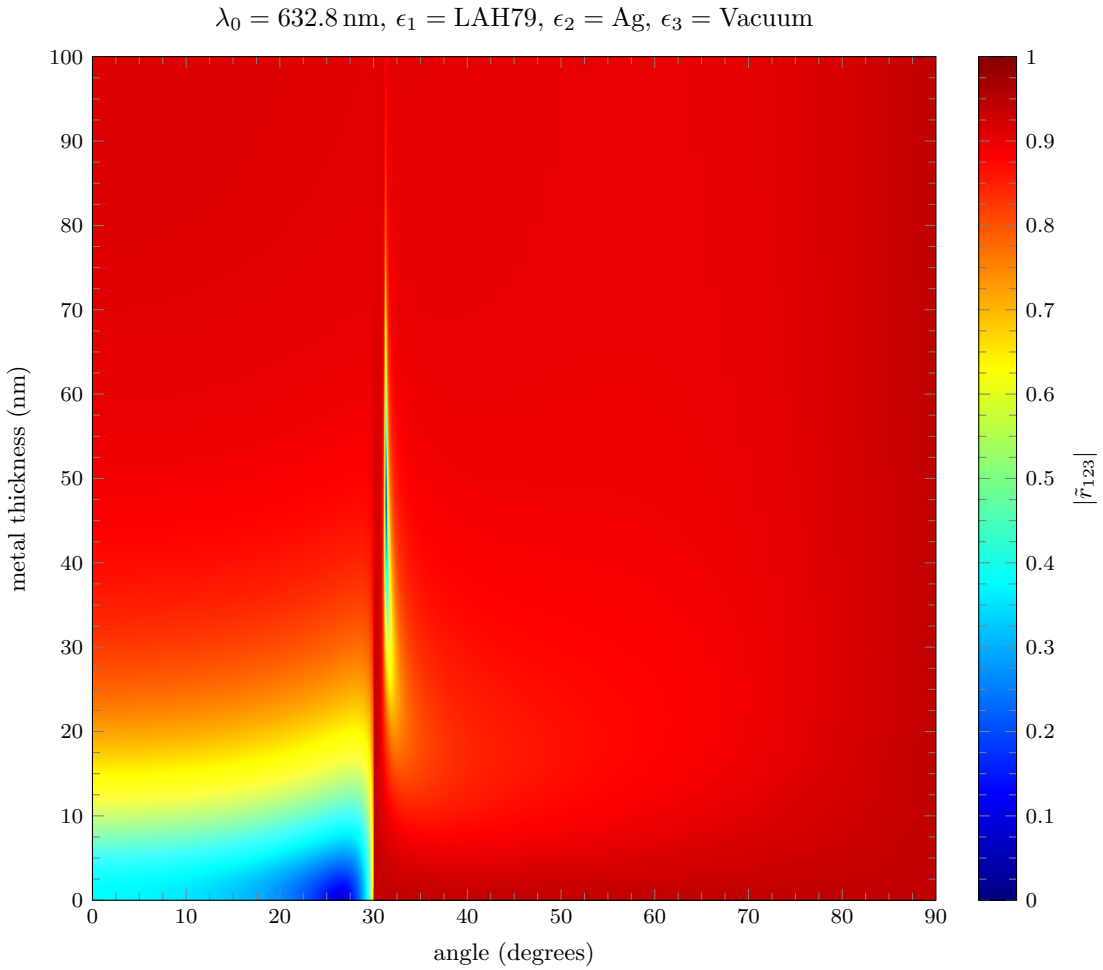

Figure 12: Reflection coefficent $|\tilde{r}_{123}|$ for the three layer fresnel system (Ag-LAH79-Vacuum) as a function of incident angle and thickness of the metal layer ϵ_2. Numeric values of the permittivity are found in Table **??**

0.2.2 Al-LAH79-Vacuum

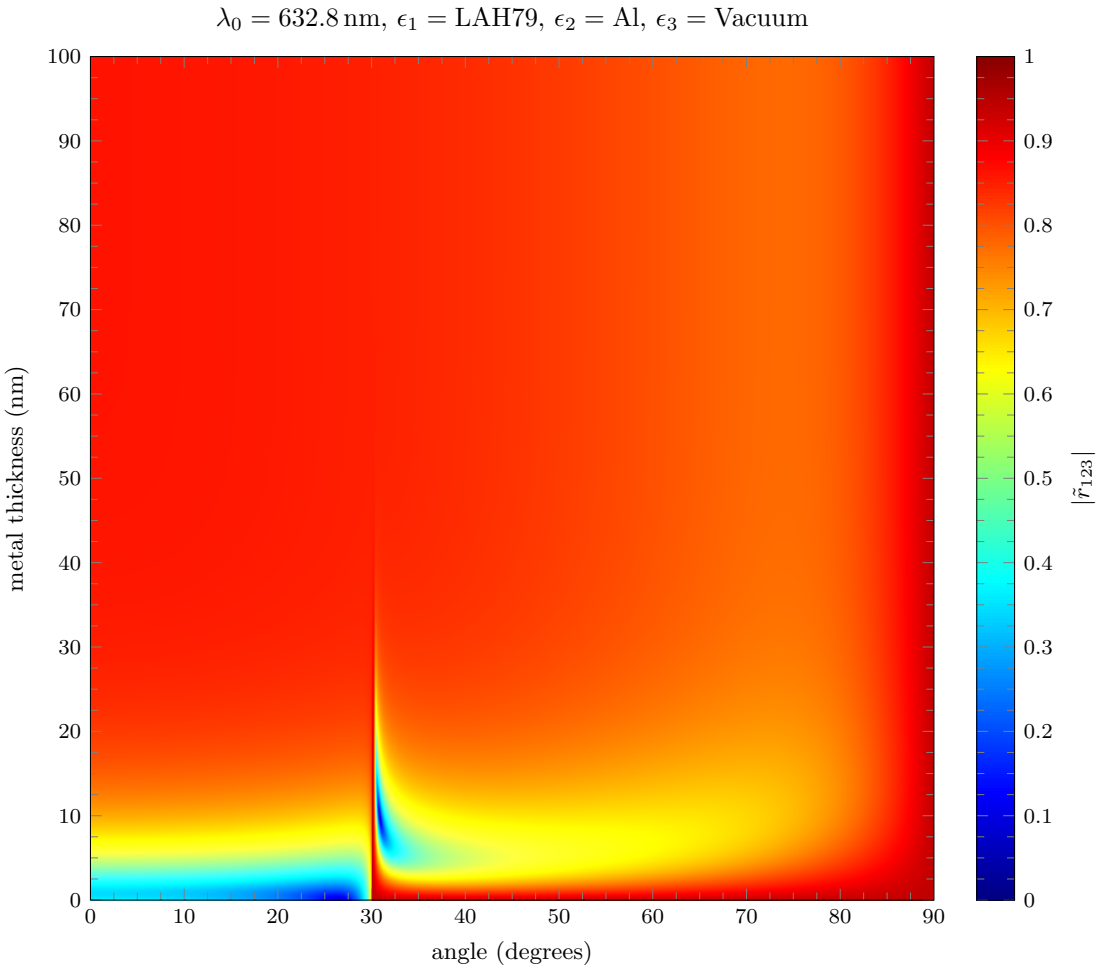

Figure 13: Reflection coefficent $|\tilde{r}_{123}|$ for the three layer fresnel system (Al-LAH79-Vacuum) as a function of incident angle and thickness of the metal layer ϵ_2. Numeric values of the permittivity are found in Table **??**

0.2.3 Au-LAH79-Vacuum

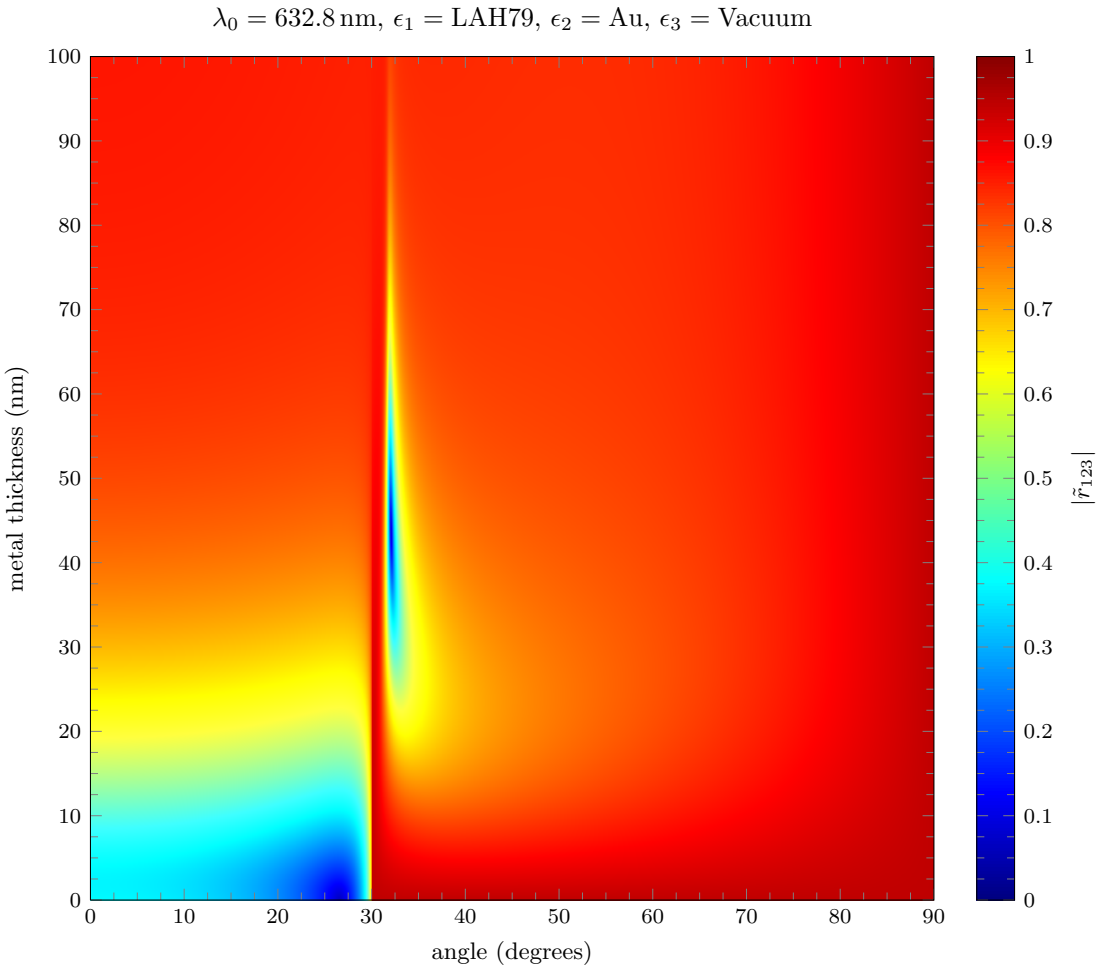

Figure 14: Reflection coefficent $|\tilde{r}_{123}|$ for the three layer fresnel system (Au-LAH79-Vacuum) as a function of incident angle and thickness of the metal layer ϵ_2. Numeric values of the permittivity are found in Table **??**

0.2.4 Be-LAH79-Vacuum

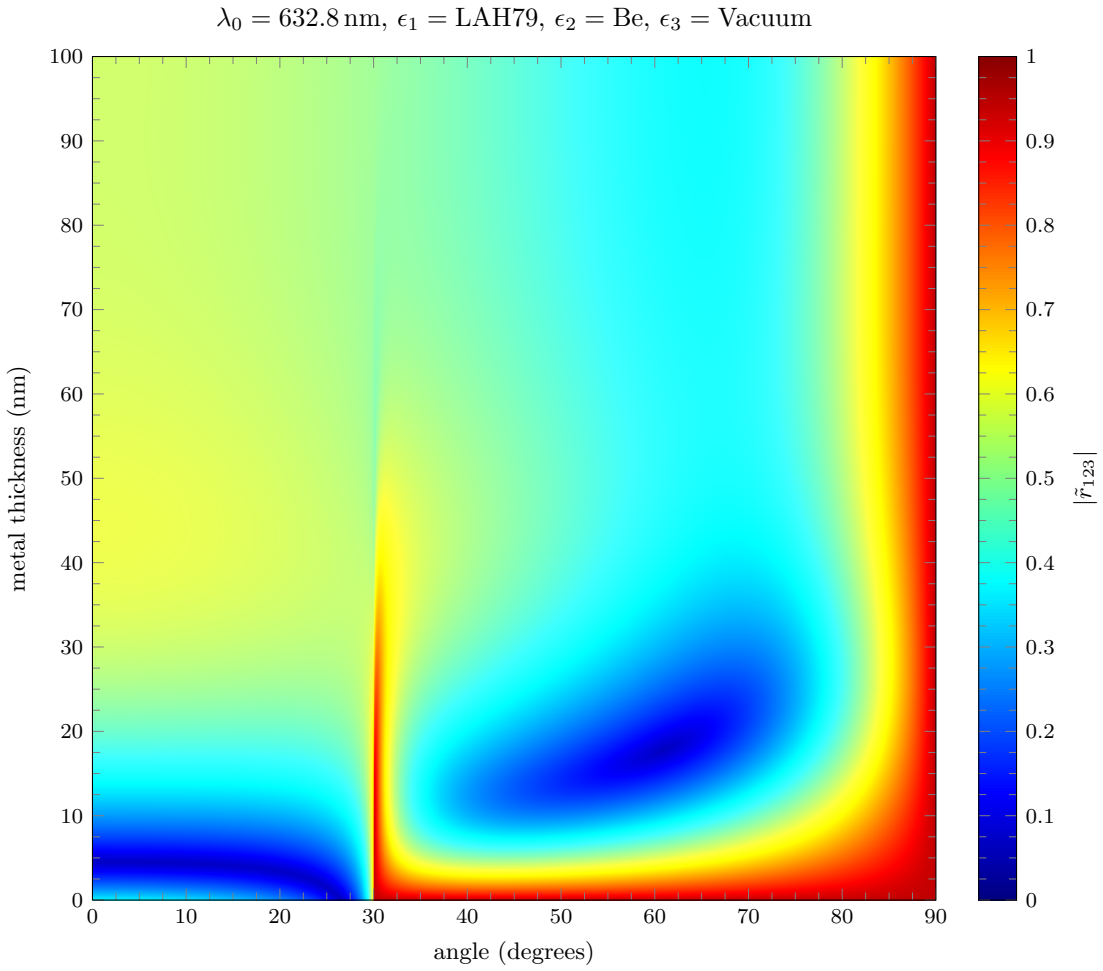

Figure 15: Reflection coefficent $|\tilde{r}_{123}|$ for the three layer fresnel system (Be-LAH79-Vacuum) as a function of incident angle and thickness of the metal layer ϵ_2. Numeric values of the permittivity are found in Table **??**

0.2.5 Cr-LAH79-Vacuum

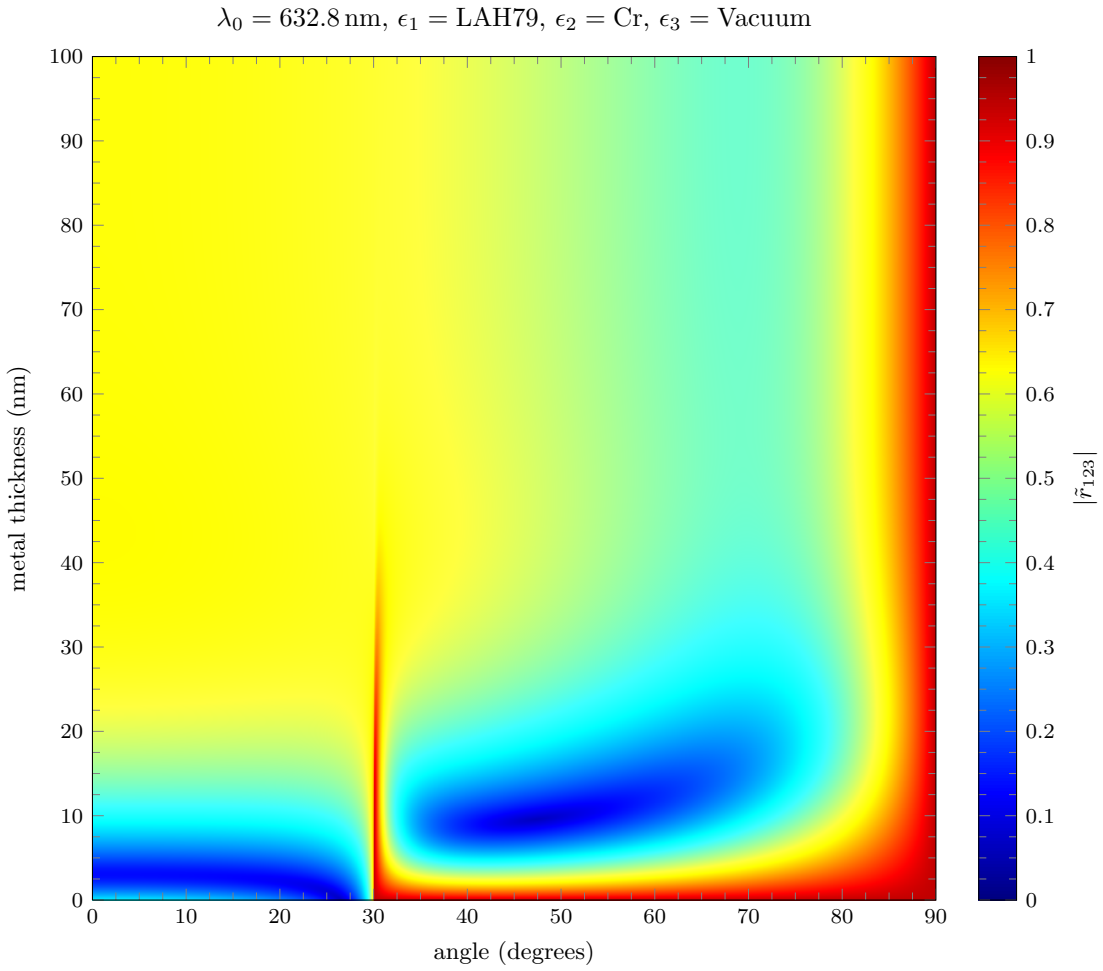

Figure 16: Reflection coefficent $|\tilde{r}_{123}|$ for the three layer fresnel system (Cr-LAH79-Vacuum) as a function of incident angle and thickness of the metal layer ϵ_2. Numeric values of the permittivity are found in Table **??**

0.2.6 Cu-LAH79-Vacuum

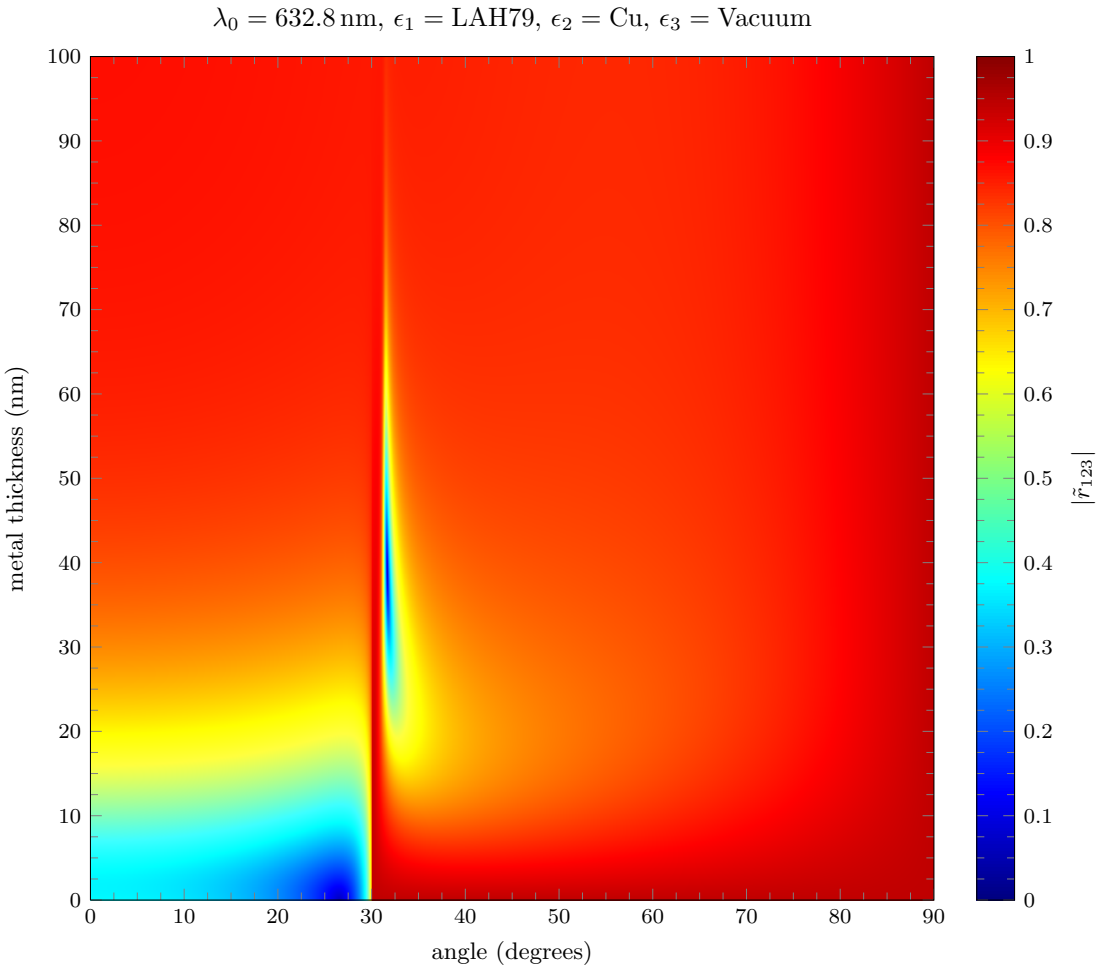

Figure 17: Reflection coefficent $|\tilde{r}_{123}|$ for the three layer fresnel system (Cu-LAH79-Vacuum) as a function of incident angle and thickness of the metal layer ϵ_2. Numeric values of the permittivity are found in Table **??**

0.2.7 Ni-LAH79-Vacuum

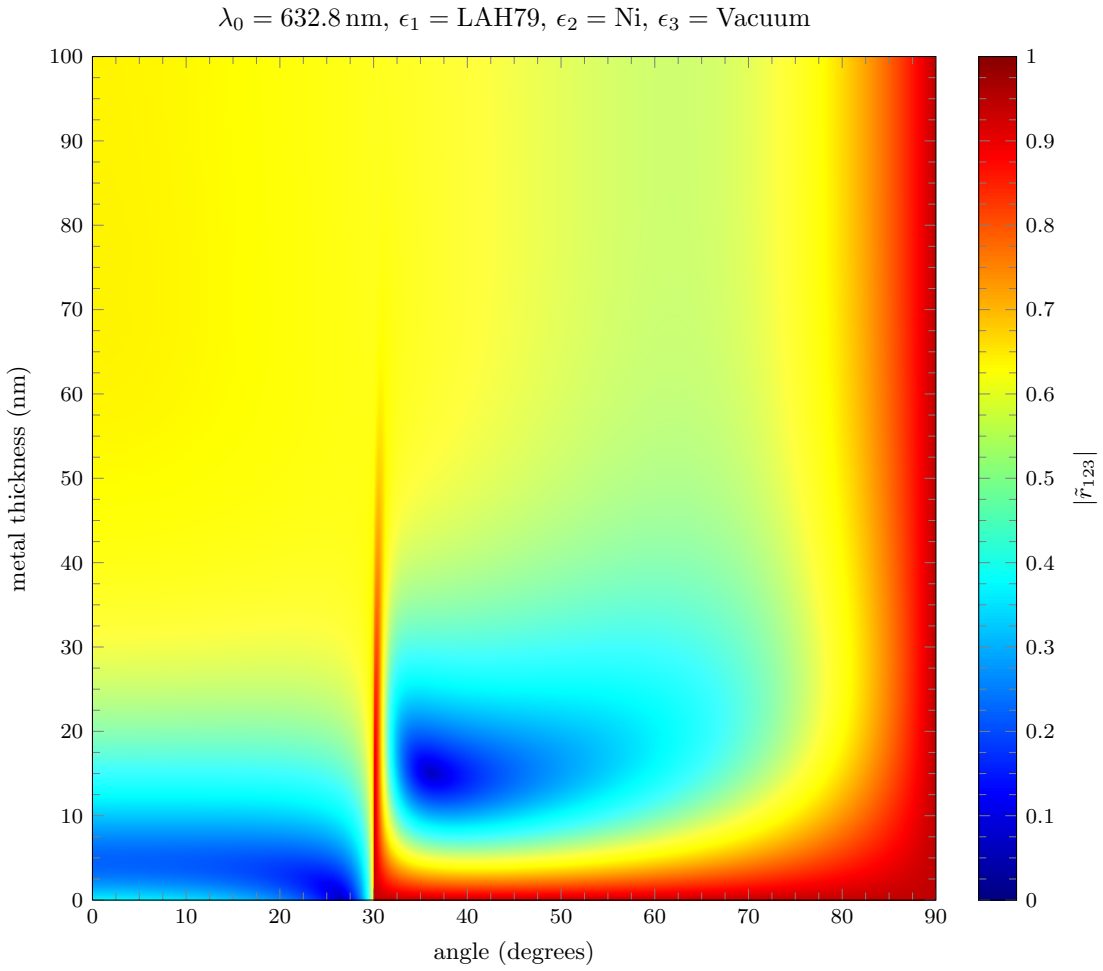

Figure 18: Reflection coefficent $|\tilde{r}_{123}|$ for the three layer fresnel system (Ni-LAH79-Vacuum) as a function of incident angle and thickness of the metal layer ϵ_2. Numeric values of the permittivity are found in Table **??**

0.2.8 Pd-LAH79-Vacuum

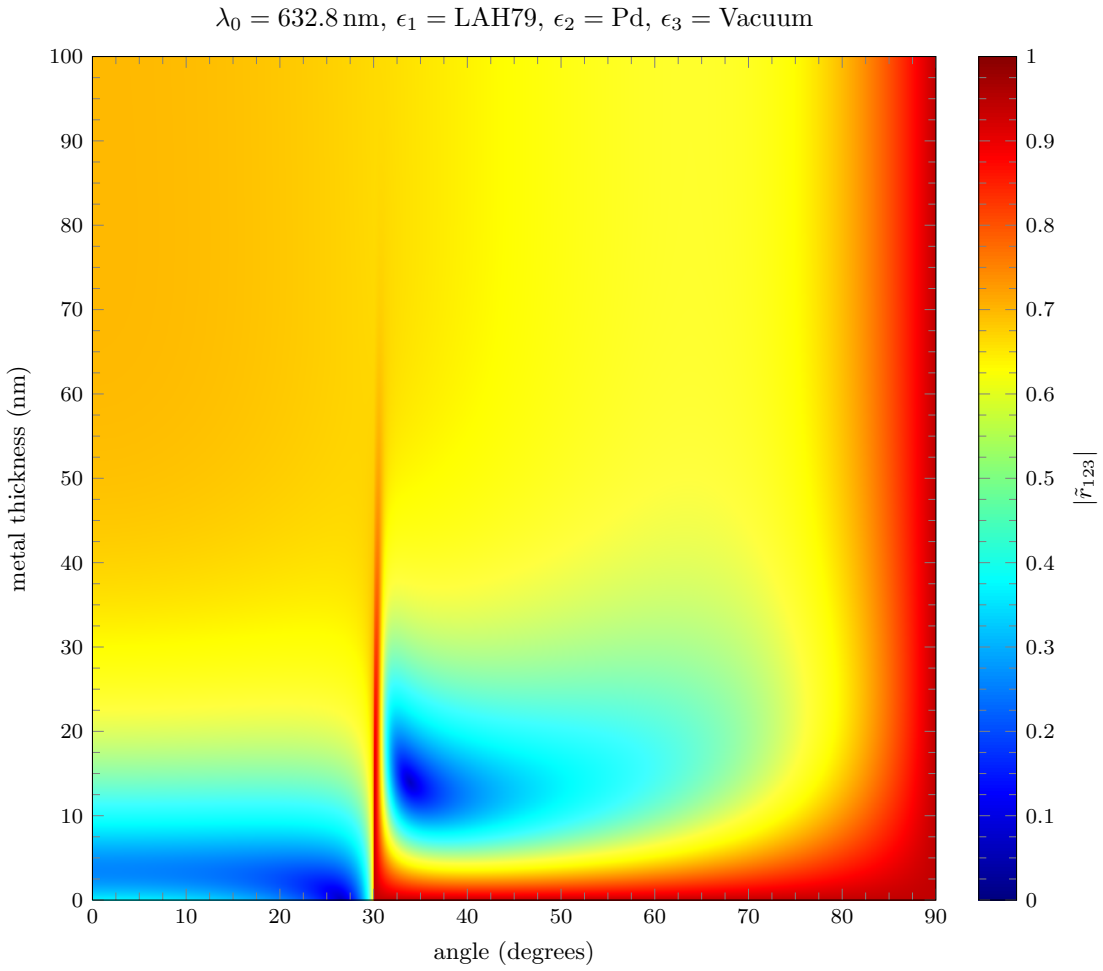

Figure 19: Reflection coefficent $|\tilde{r}_{123}|$ for the three layer fresnel system (Pd-LAH79-Vacuum) as a function of incident angle and thickness of the metal layer ϵ_2. Numeric values of the permittivity are found in Table **??**

0.2.9 Pt-LAH79-Vacuum

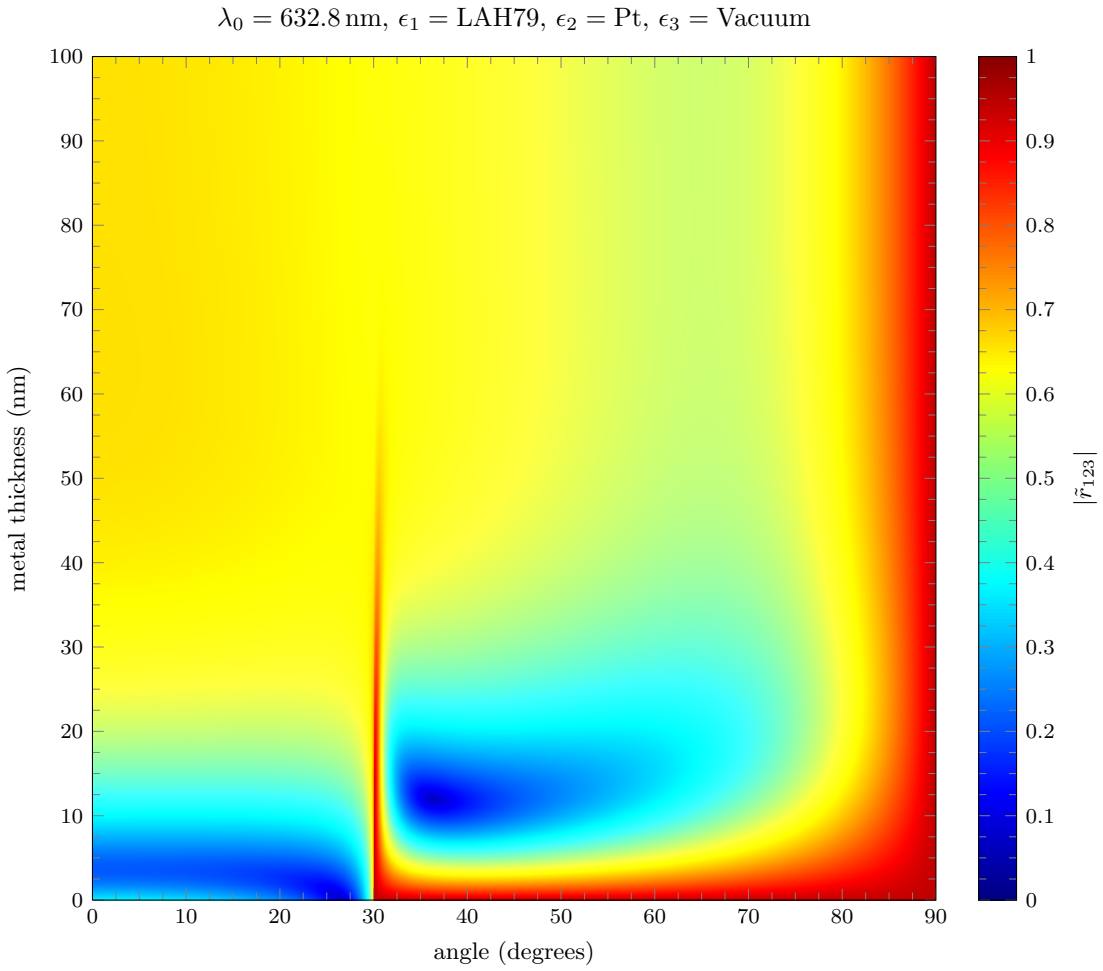

Figure 20: Reflection coefficent $|\tilde{r}_{123}|$ for the three layer fresnel system (Pt-LAH79-Vacuum) as a function of incident angle and thickness of the metal layer ϵ_2. Numeric values of the permittivity are found in Table **??**

0.2.10 Ti-LAH79-Vacuum

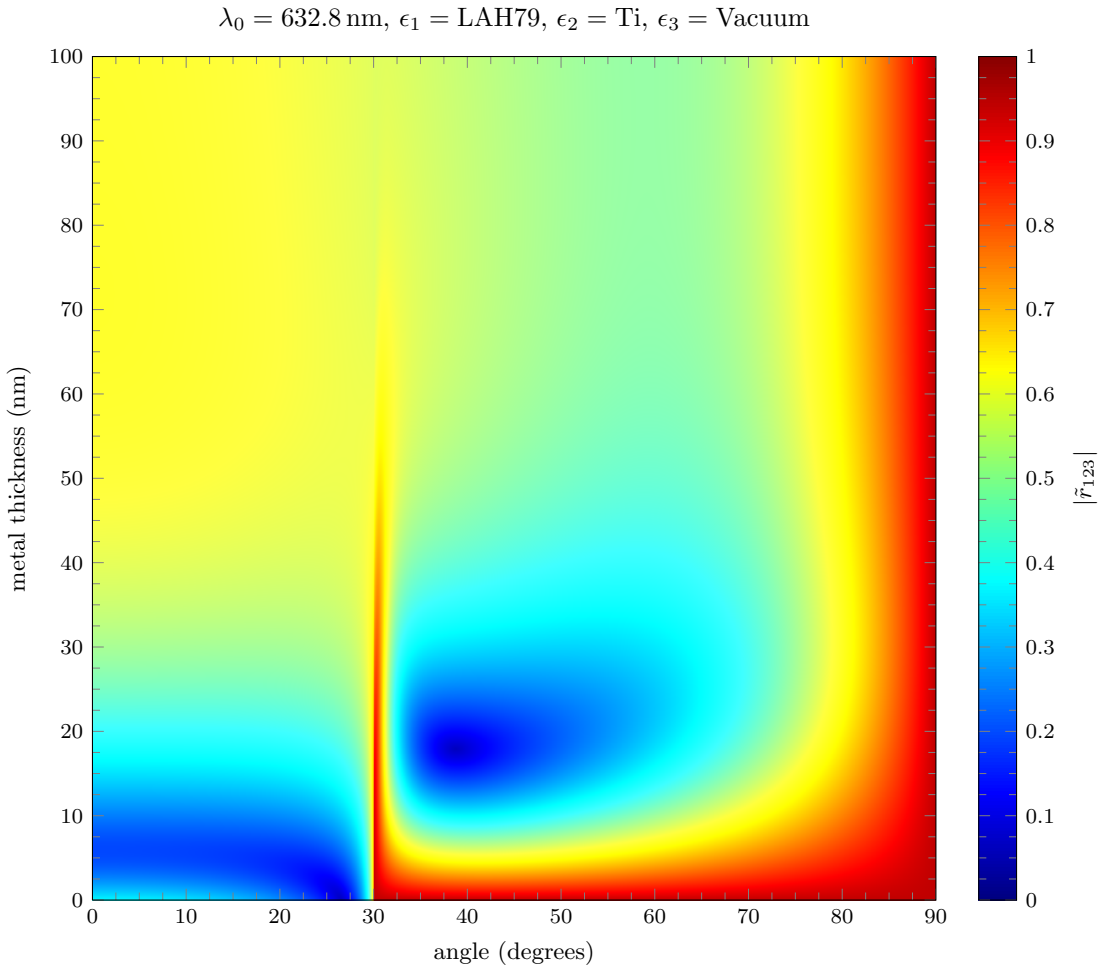

Figure 21: Reflection coefficent $|\tilde{r}_{123}|$ for the three layer fresnel system (Ti-LAH79-Vacuum) as a function of incident angle and thickness of the metal layer ϵ_2. Numeric values of the permittivity are found in Table **??**

0.2.11 W-LAH79-Vacuum

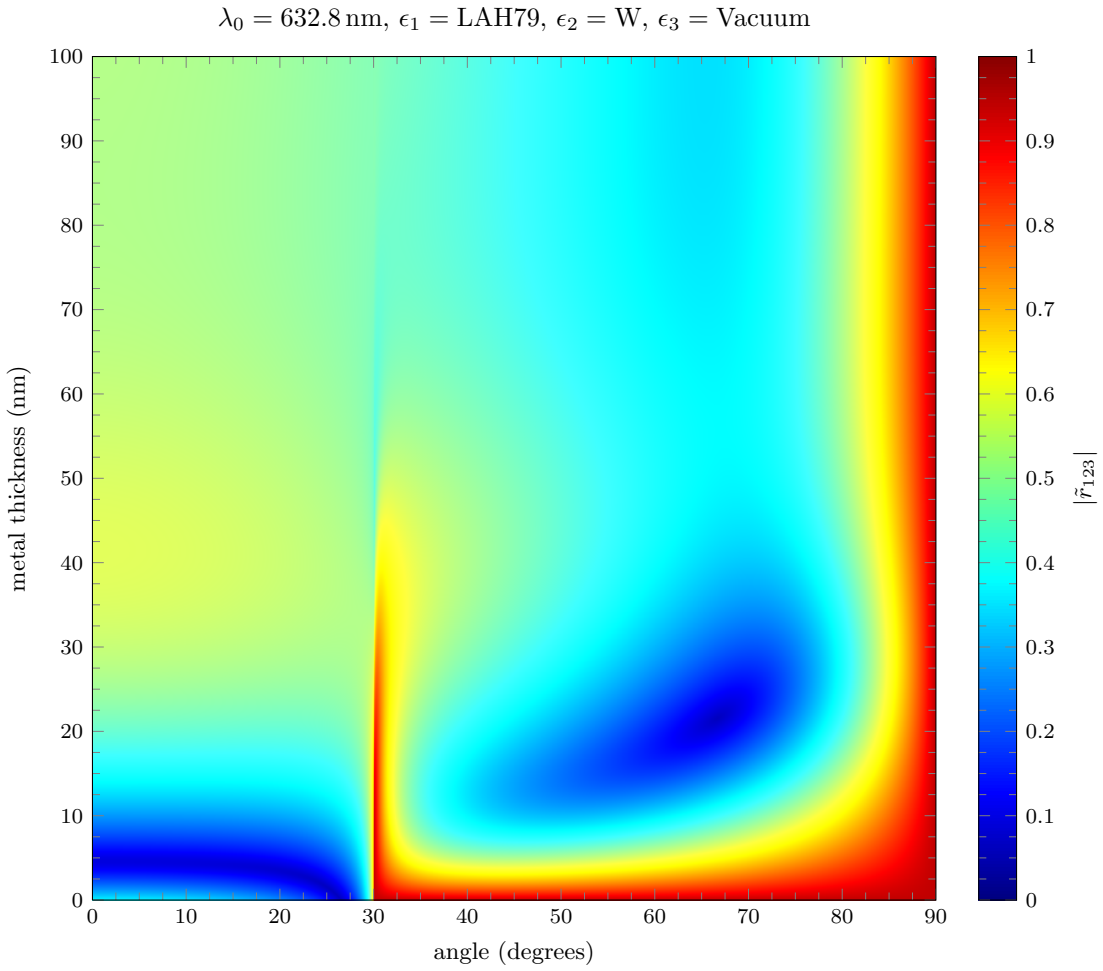

Figure 22: Reflection coefficent $|\tilde{r}_{123}|$ for the three layer fresnel system (W-LAH79-Vacuum) as a function of incident angle and thickness of the metal layer ϵ_2. Numeric values of the permittivity are found in Table **??**

0.3 Metal-BK7-H_2O

0.3.1 Ag-BK7-H_2O

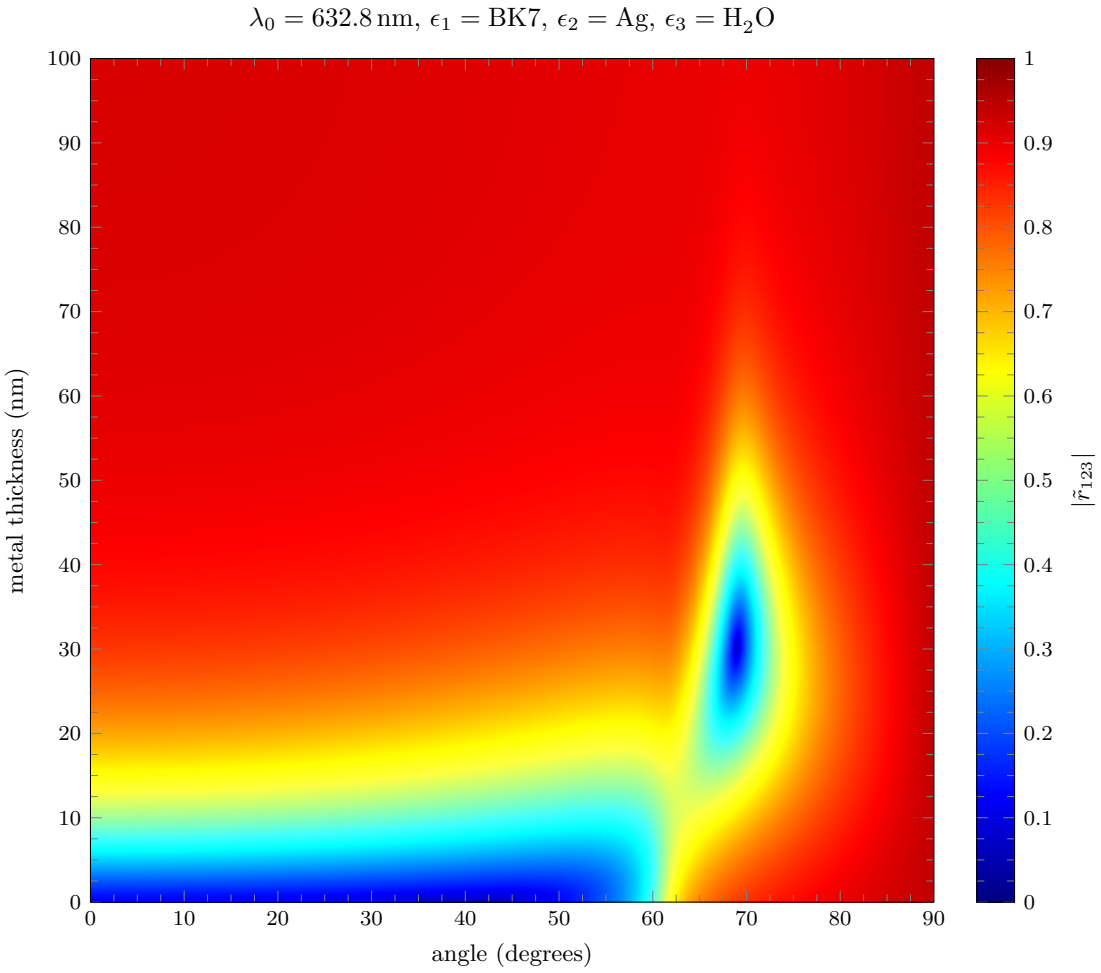

Figure 23: Reflection coefficent $|\tilde{r}_{123}|$ for the three layer fresnel system (Ag-BK7-H_2O) as a function of incident angle and thickness of the metal layer ϵ_2. Numeric values of the permittivity are found in Table **??**

0.3.2 Al-BK7-H_2O

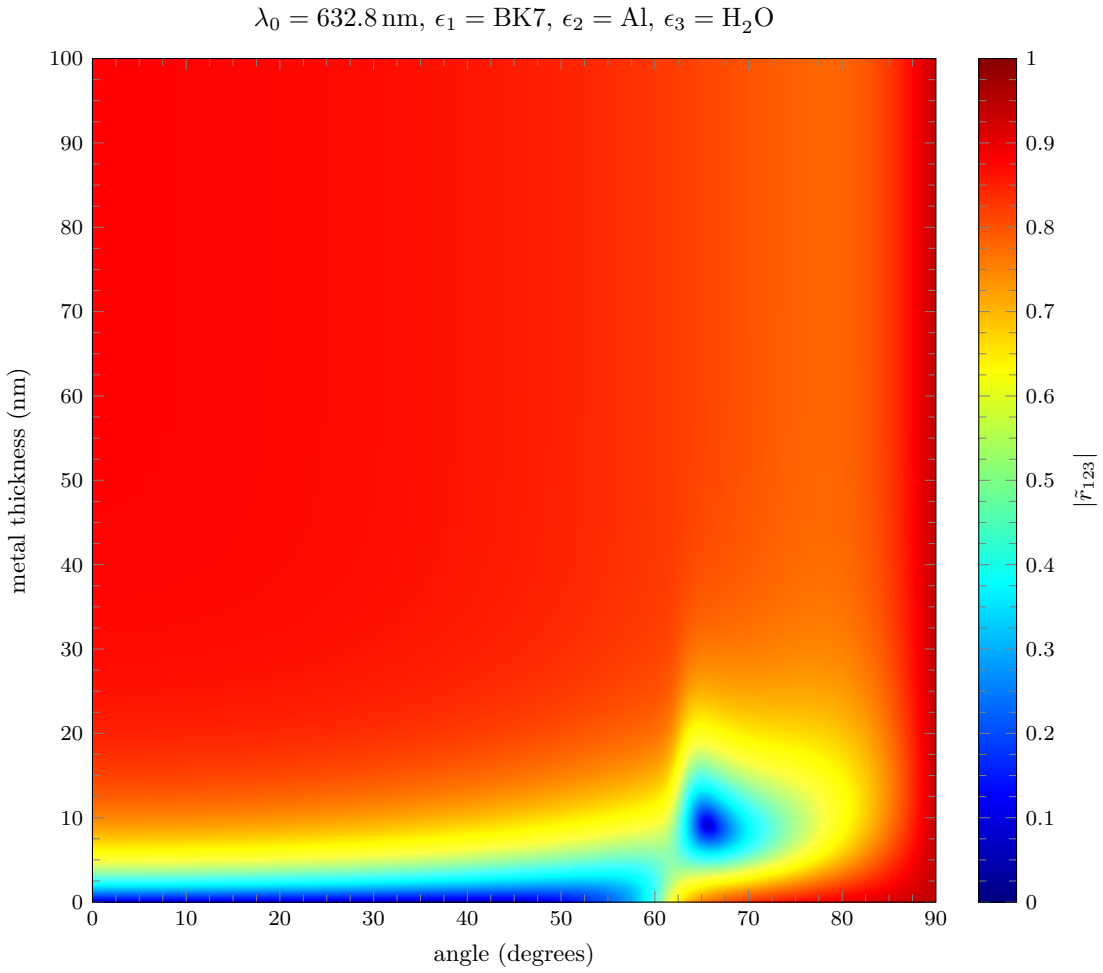

Figure 24: Reflection coefficent $|\tilde{r}_{123}|$ for the three layer fresnel system (Al-BK7-H_2O) as a function of incident angle and thickness of the metal layer ϵ_2. Numeric values of the permittivity are found in Table **??**

0.3.3 Au-BK7-H_2O

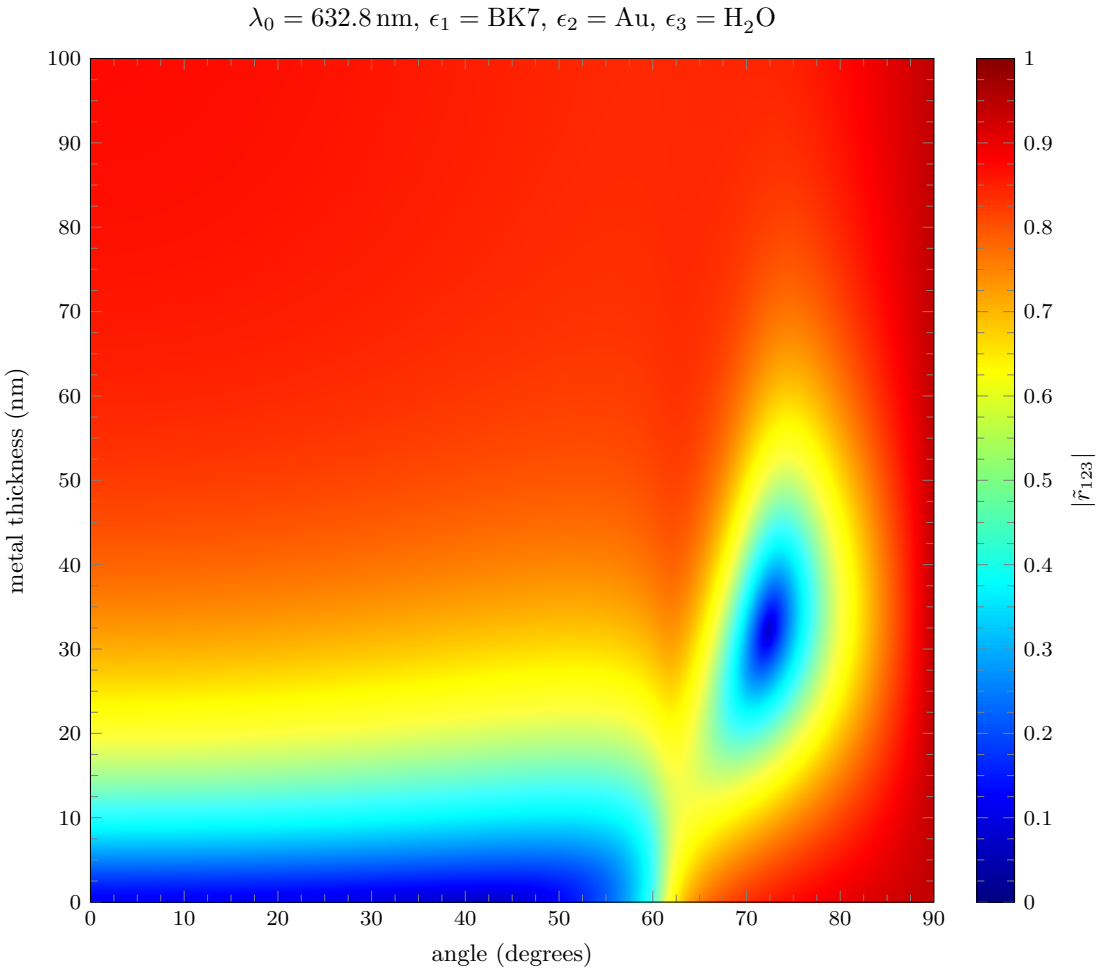

Figure 25: Reflection coefficent $|\tilde{r}_{123}|$ for the three layer fresnel system (Au-BK7-H_2O) as a function of incident angle and thickness of the metal layer ϵ_2. Numeric values of the permittivity are found in Table **??**

0.3.4 Be-BK7-H_2O

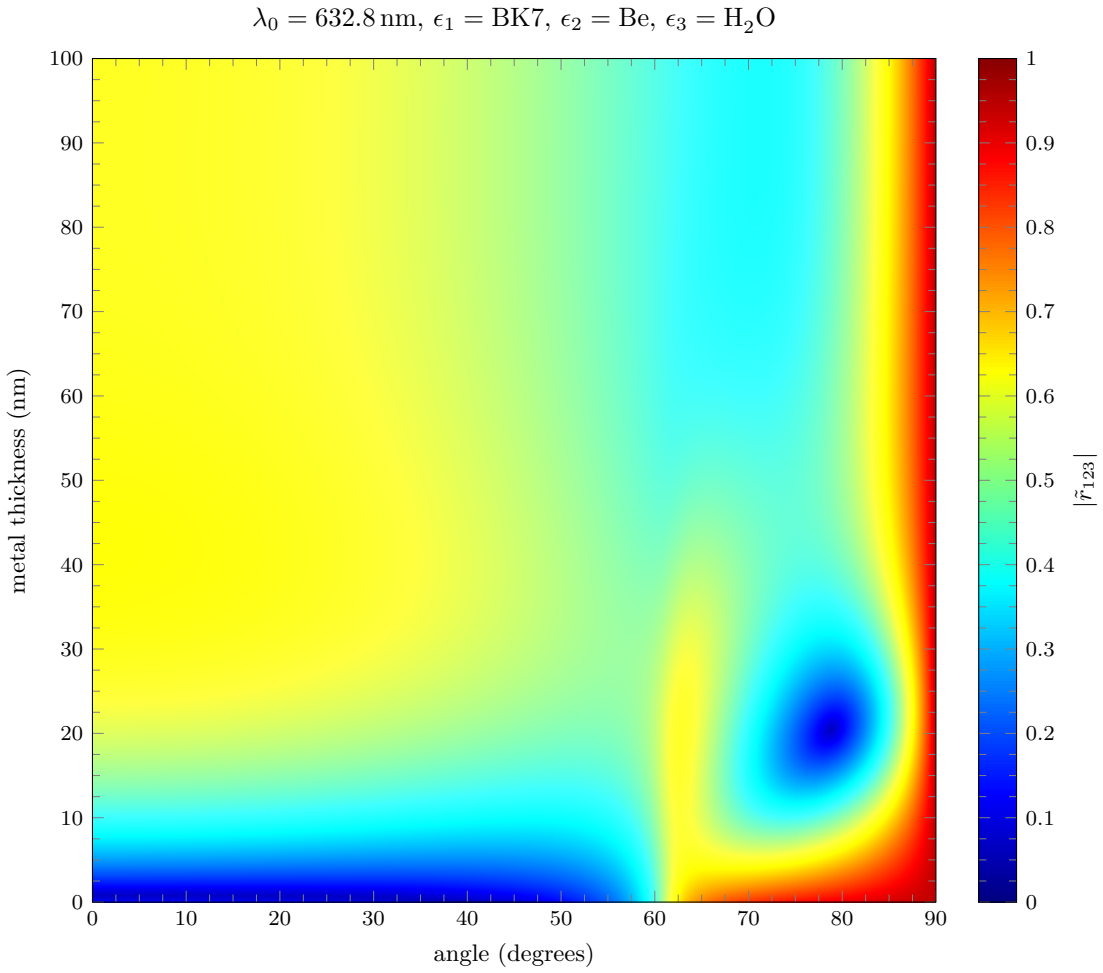

Figure 26: Reflection coefficent $|\tilde{r}_{123}|$ for the three layer fresnel system (Be-BK7-H_2O) as a function of incident angle and thickness of the metal layer ϵ_2. Numeric values of the permittivity are found in Table **??**

0.3.5 Cr-BK7-H_2O

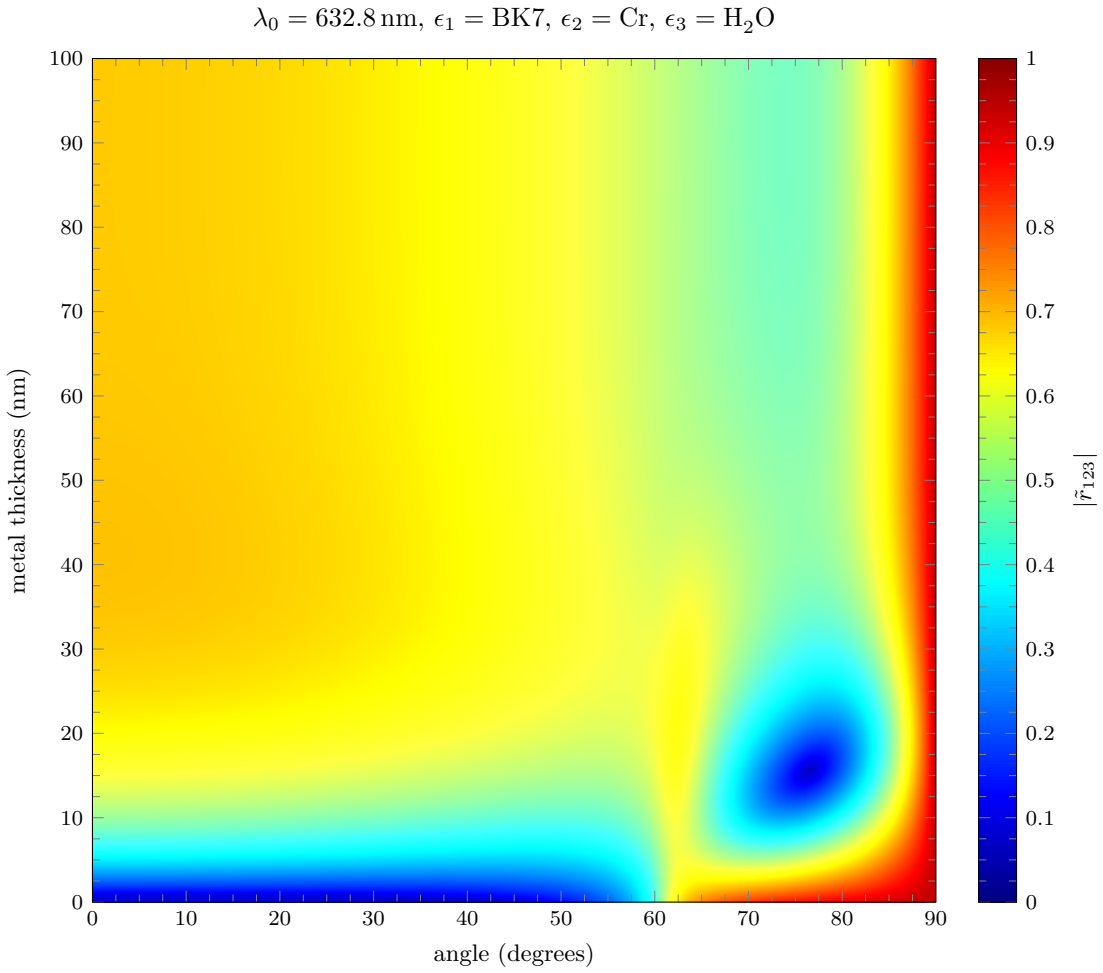

Figure 27: Reflection coefficent $|\tilde{r}_{123}|$ for the three layer fresnel system (Cr-BK7-H_2O) as a function of incident angle and thickness of the metal layer ϵ_2. Numeric values of the permittivity are found in Table **??**

0.3.6 Cu-BK7-H_2O

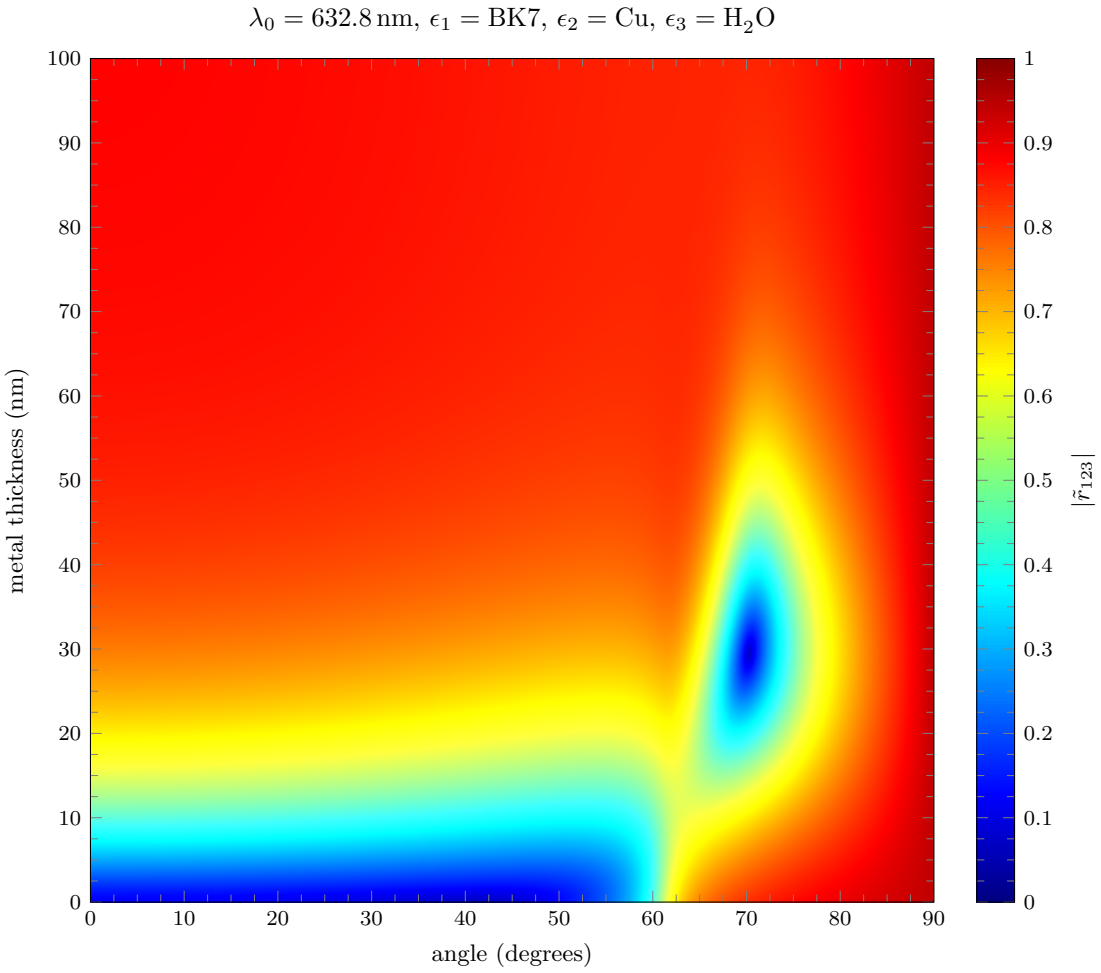

Figure 28: Reflection coefficent $|\tilde{r}_{123}|$ for the three layer fresnel system (Cu-BK7-H_2O) as a function of incident angle and thickness of the metal layer ϵ_2. Numeric values of the permittivity are found in Table **??**

0.3.7 Ni-BK7-H_2O

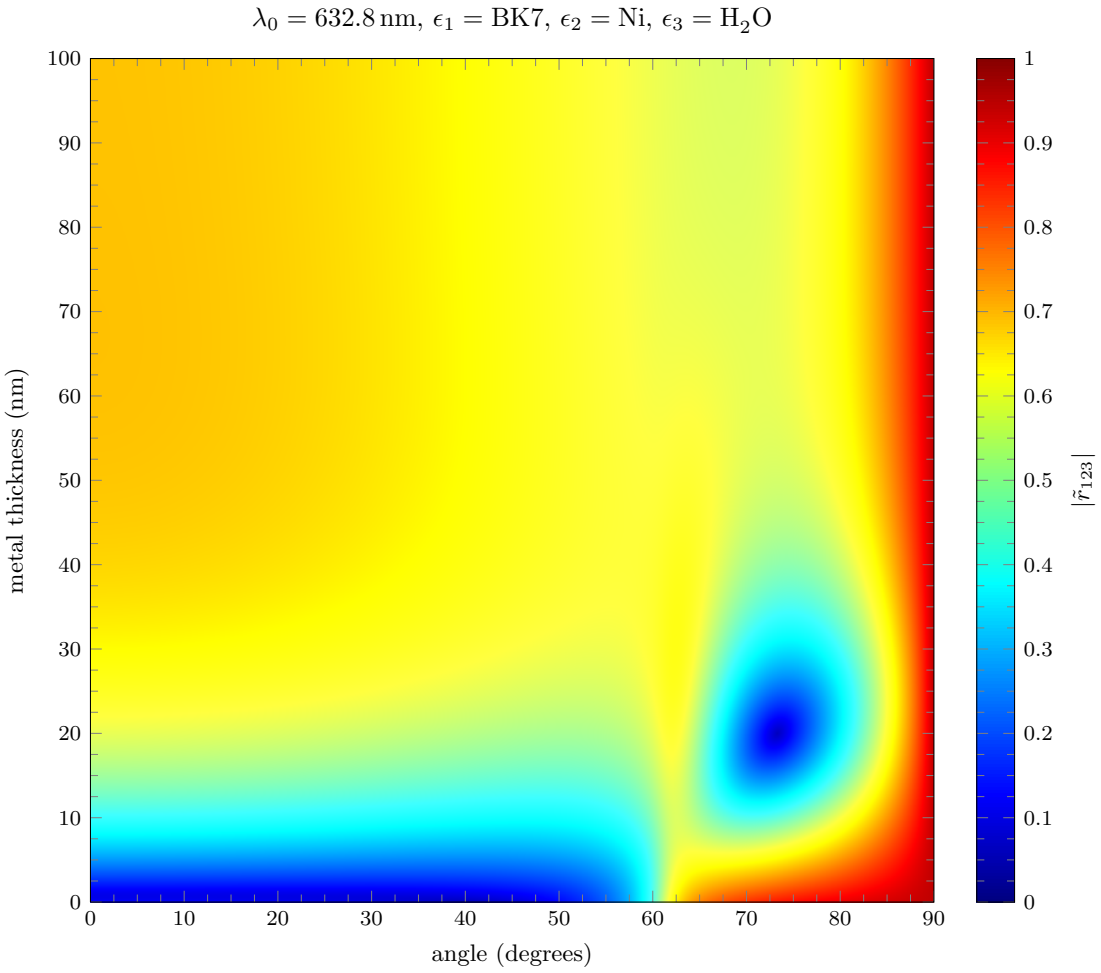

Figure 29: Reflection coefficent $|\tilde{r}_{123}|$ for the three layer fresnel system (Ni-BK7-H_2O) as a function of incident angle and thickness of the metal layer ϵ_2. Numeric values of the permittivity are found in Table **??**

0.3.8 Pd-BK7-H_2O

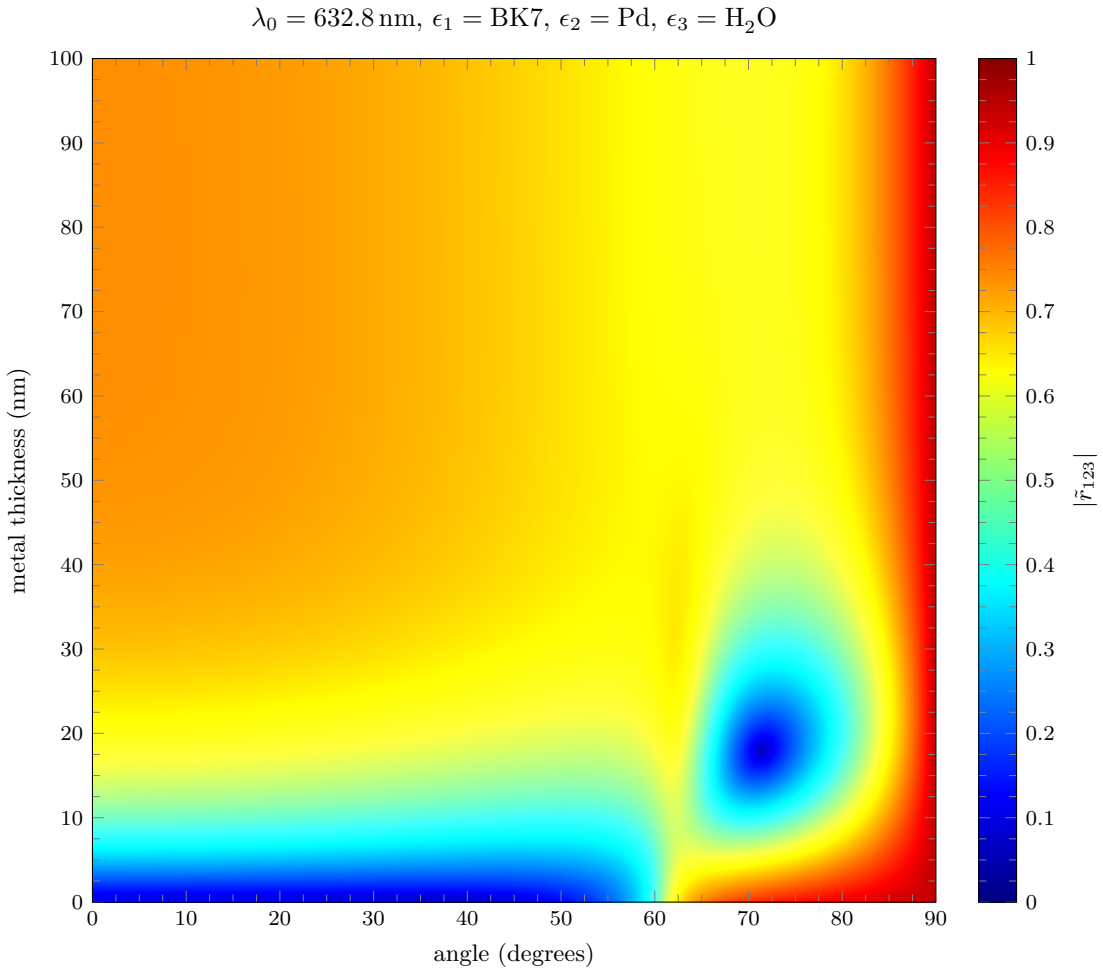

Figure 30: Reflection coefficent $|\tilde{r}_{123}|$ for the three layer fresnel system (Pd-BK7-H_2O) as a function of incident angle and thickness of the metal layer ϵ_2. Numeric values of the permittivity are found in Table **??**

0.3.9 Pt-BK7-H_2O

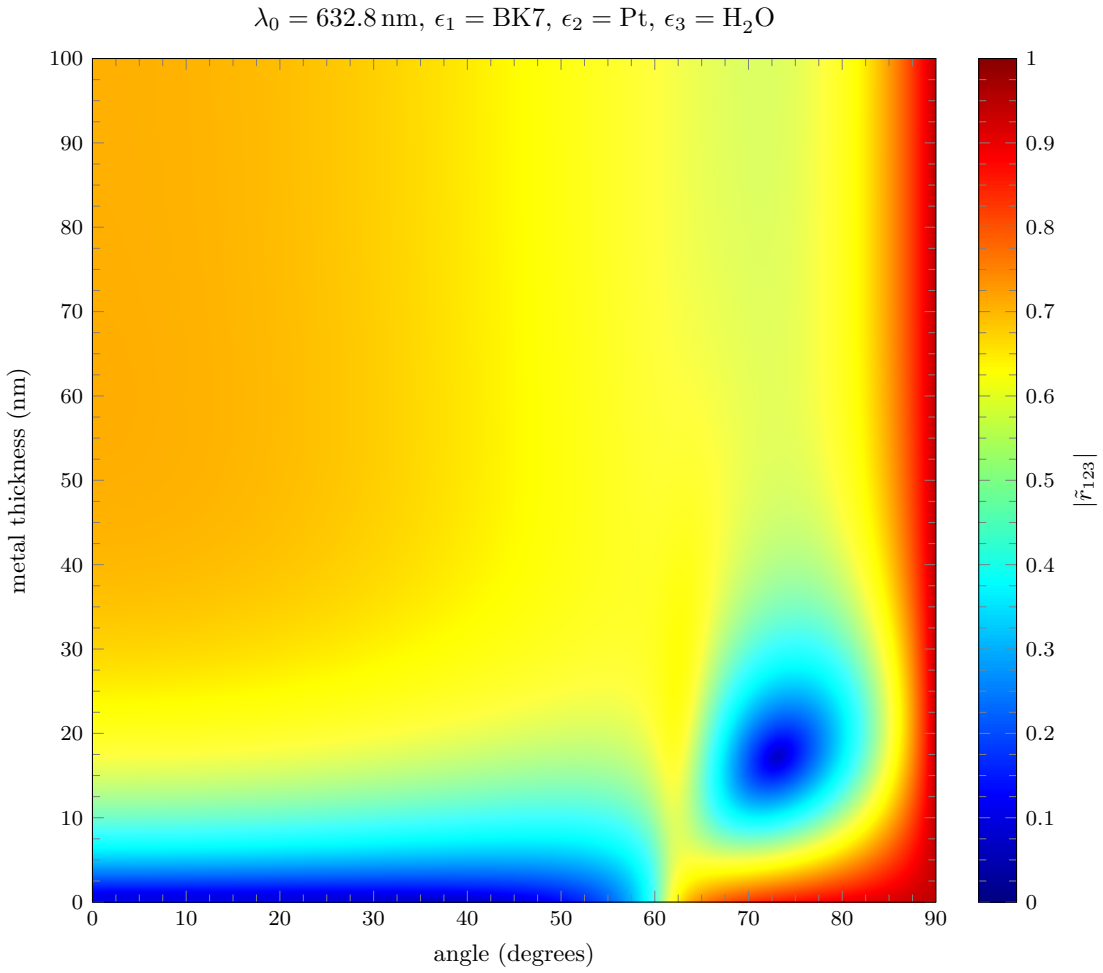

Figure 31: Reflection coefficent $|\tilde{r}_{123}|$ for the three layer fresnel system (Pt-BK7-H_2O) as a function of incident angle and thickness of the metal layer ϵ_2. Numeric values of the permittivity are found in Table **??**

0.3.10 Ti-BK7-H_2O

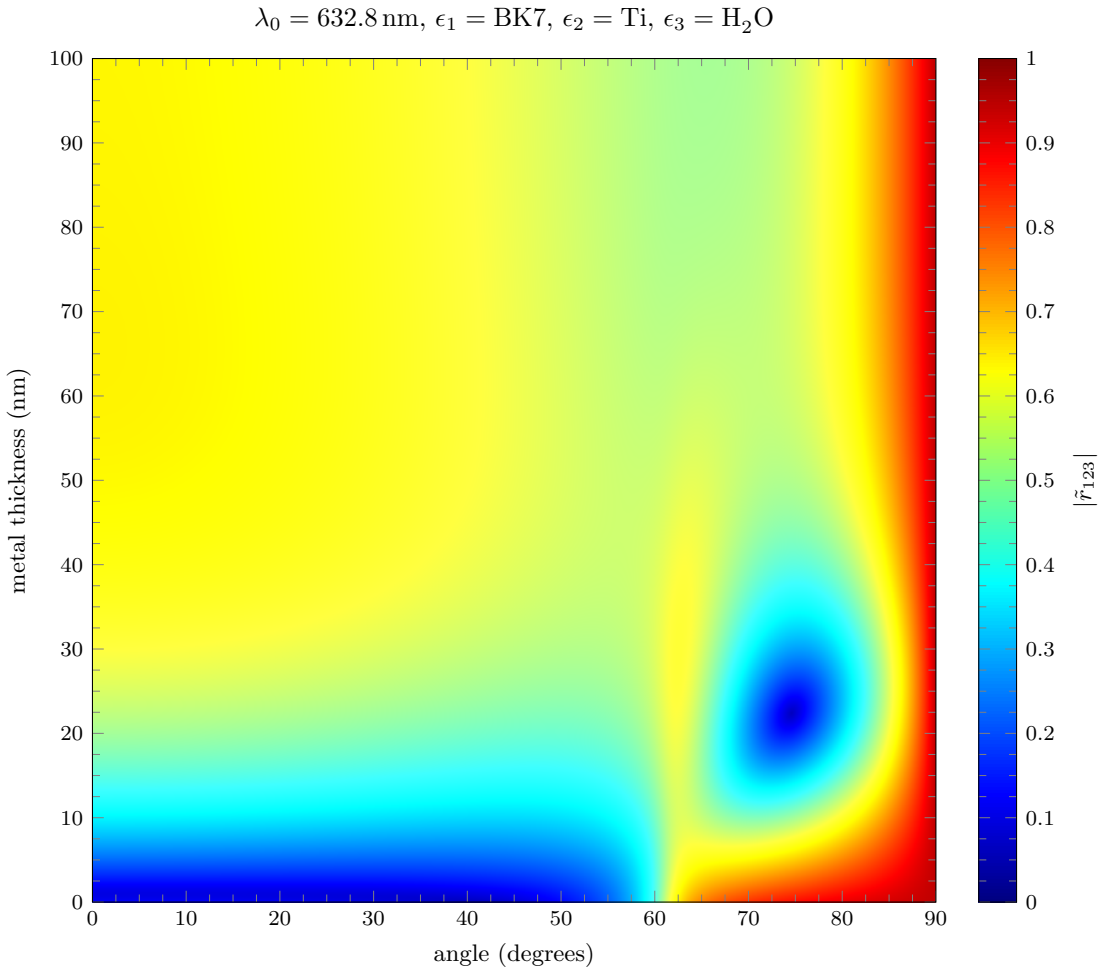

Figure 32: Reflection coefficent $|\tilde{r}_{123}|$ for the three layer fresnel system (Ti-BK7-H_2O) as a function of incident angle and thickness of the metal layer ϵ_2. Numeric values of the permittivity are found in Table **??**

0.3.11 W-BK7-H_2O

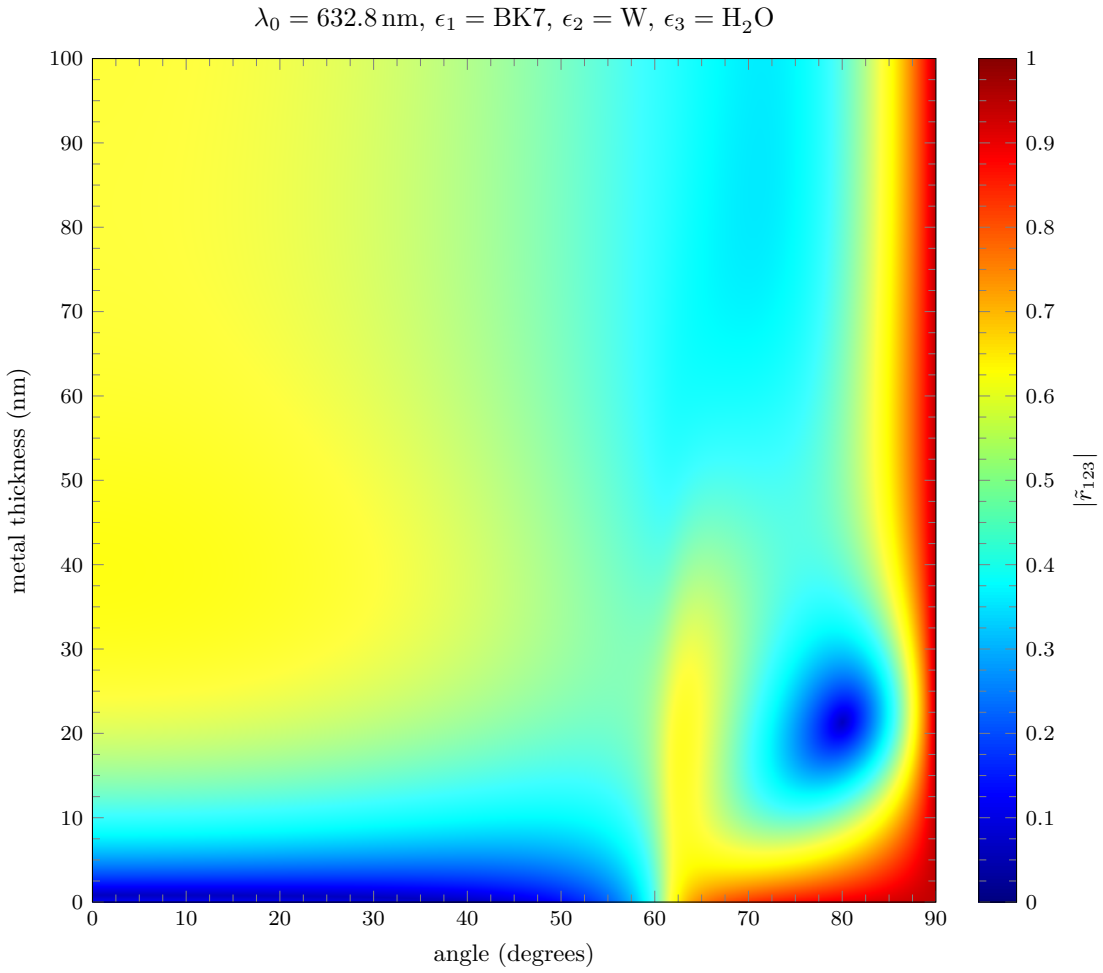

Figure 33: Reflection coefficent $|\tilde{r}_{123}|$ for the three layer fresnel system (W-BK7-H_2O) as a function of incident angle and thickness of the metal layer ϵ_2. Numeric values of the permittivity are found in Table **??**

0.4 Metal-LAH79-H_2O

0.4.1 Ag-LAH79-H_2O

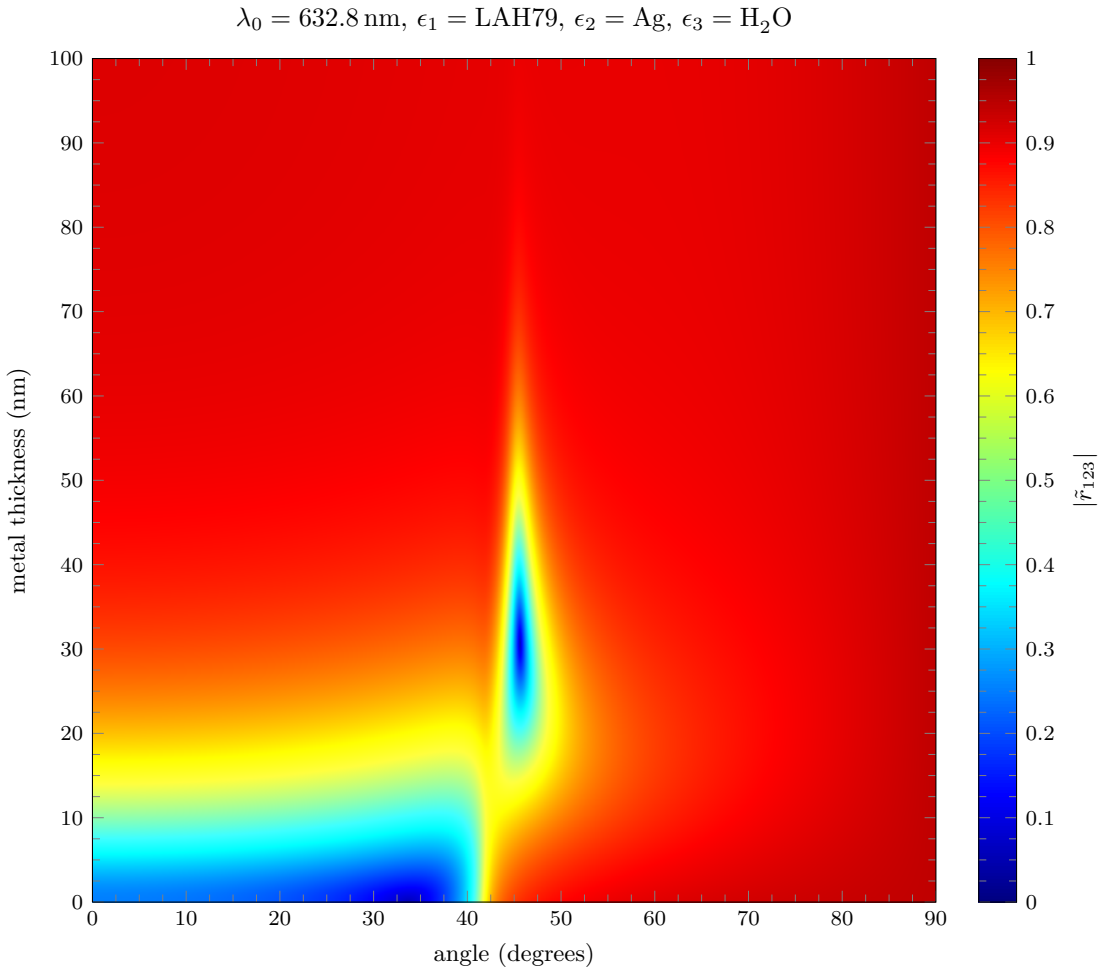

Figure 34: Reflection coefficent $|\tilde{r}_{123}|$ for the three layer fresnel system (Ag-LAH79-H_2O) as a function of incident angle and thickness of the metal layer ϵ_2. Numeric values of the permittivity are found in Table **??**

0.4.2 Al-LAH79-H_2O

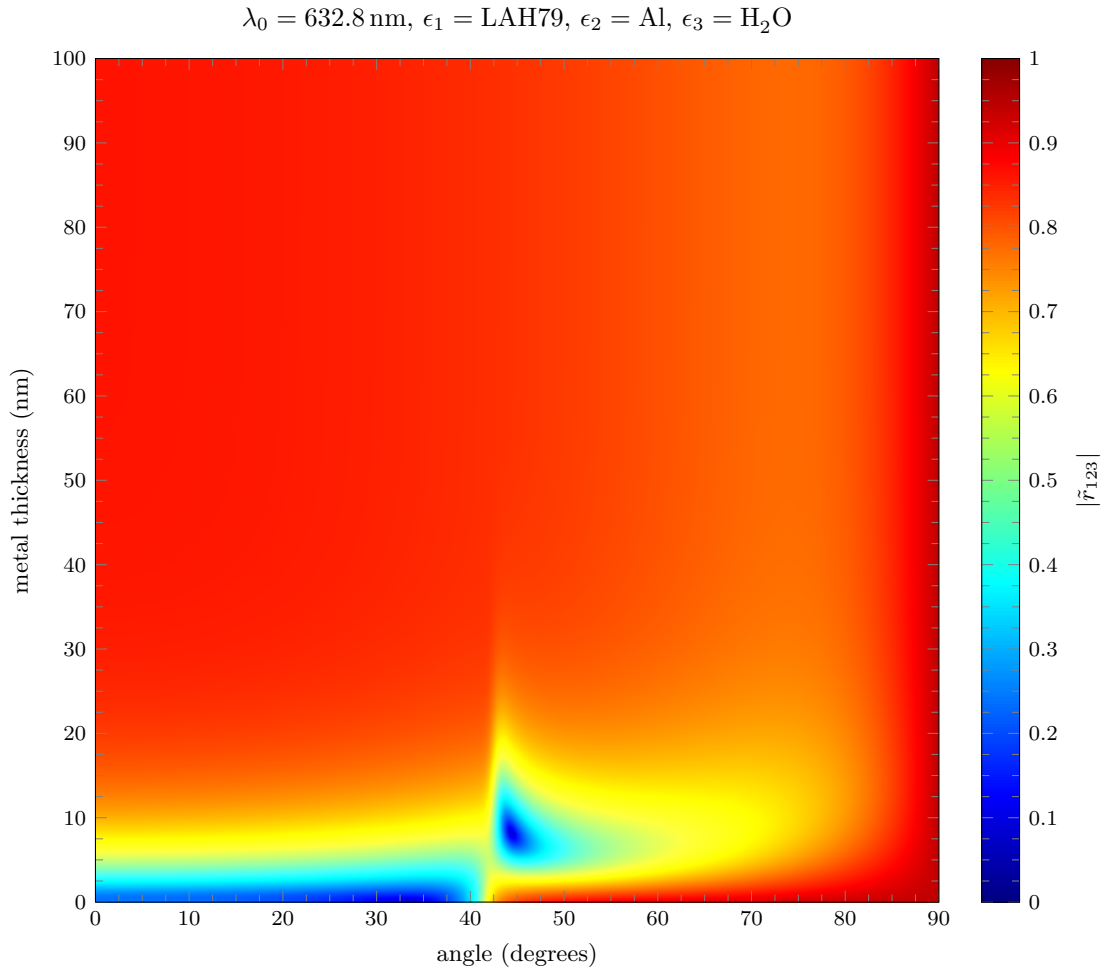

Figure 35: Reflection coefficent $|\tilde{r}_{123}|$ for the three layer fresnel system (Al-LAH79-H_2O) as a function of incident angle and thickness of the metal layer ϵ_2. Numeric values of the permittivity are found in Table **??**

0.4.3 Au-LAH79-H_2O

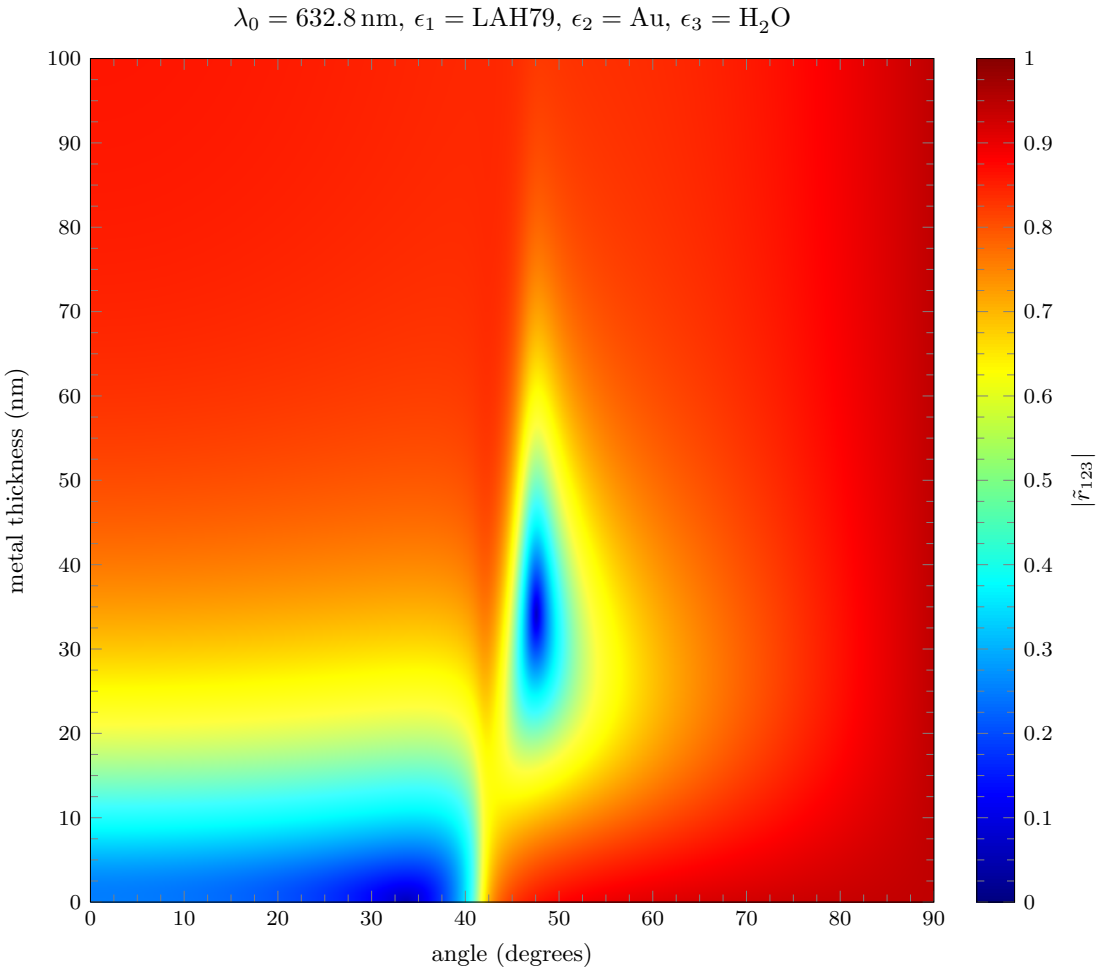

Figure 36: Reflection coefficent $|\tilde{r}_{123}|$ for the three layer fresnel system (Au-LAH79-H_2O) as a function of incident angle and thickness of the metal layer ϵ_2. Numeric values of the permittivity are found in Table **??**

0.4.4 Be-LAH79-H_2O

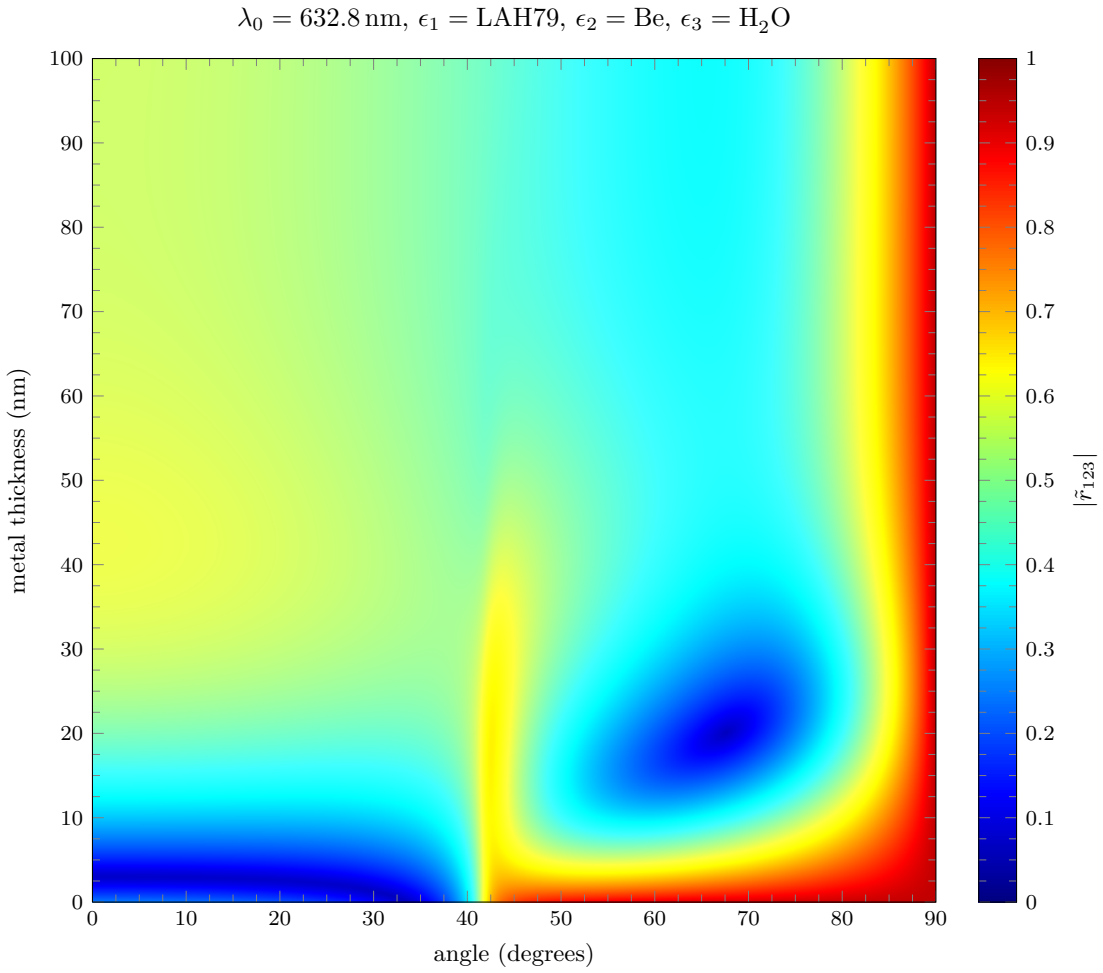

Figure 37: Reflection coefficent $|\tilde{r}_{123}|$ for the three layer fresnel system (Be-LAH79-H_2O) as a function of incident angle and thickness of the metal layer ϵ_2. Numeric values of the permittivity are found in Table **??**

0.4.5 Cr-LAH79-H_2O

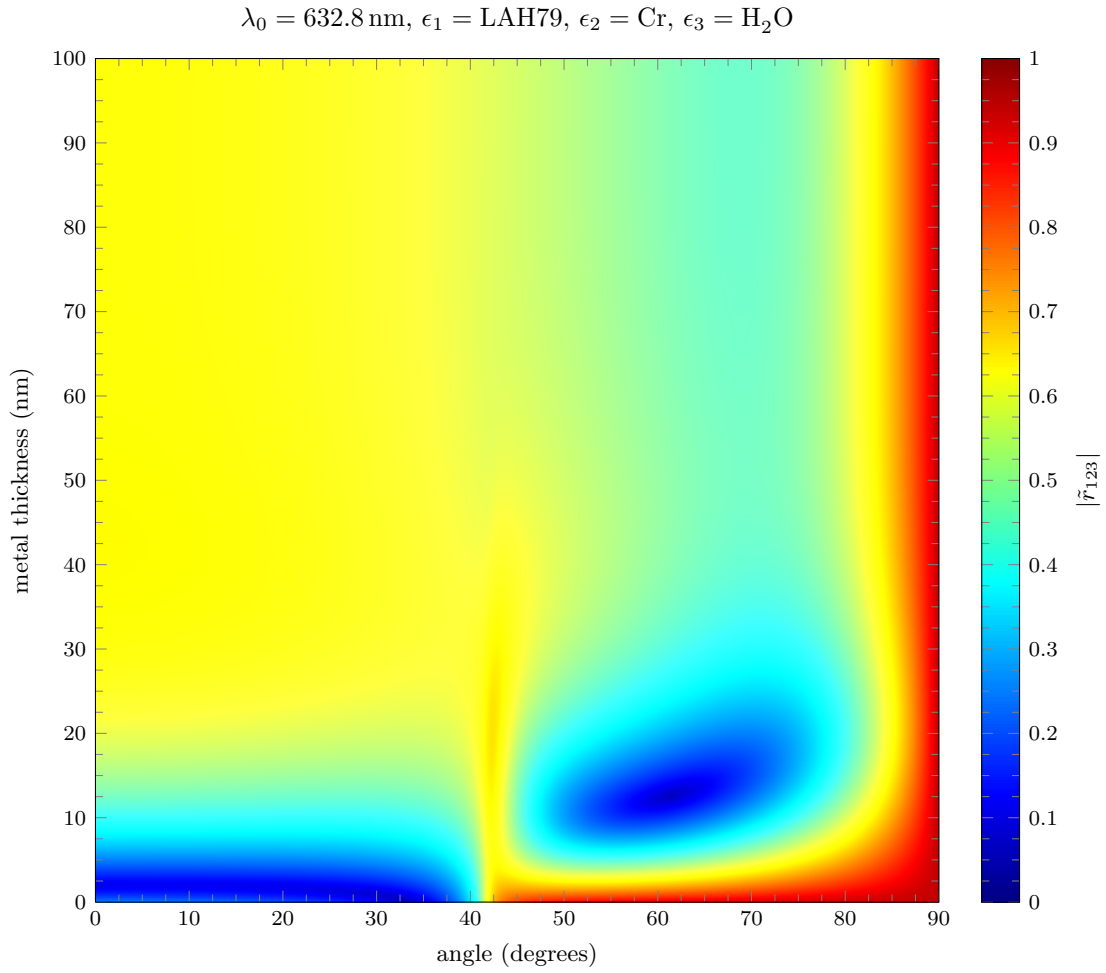

Figure 38: Reflection coefficent $|\tilde{r}_{123}|$ for the three layer fresnel system (Cr-LAH79-H_2O) as a function of incident angle and thickness of the metal layer ϵ_2. Numeric values of the permittivity are found in Table **??**

0.4.6 Cu-LAH79-H_2O

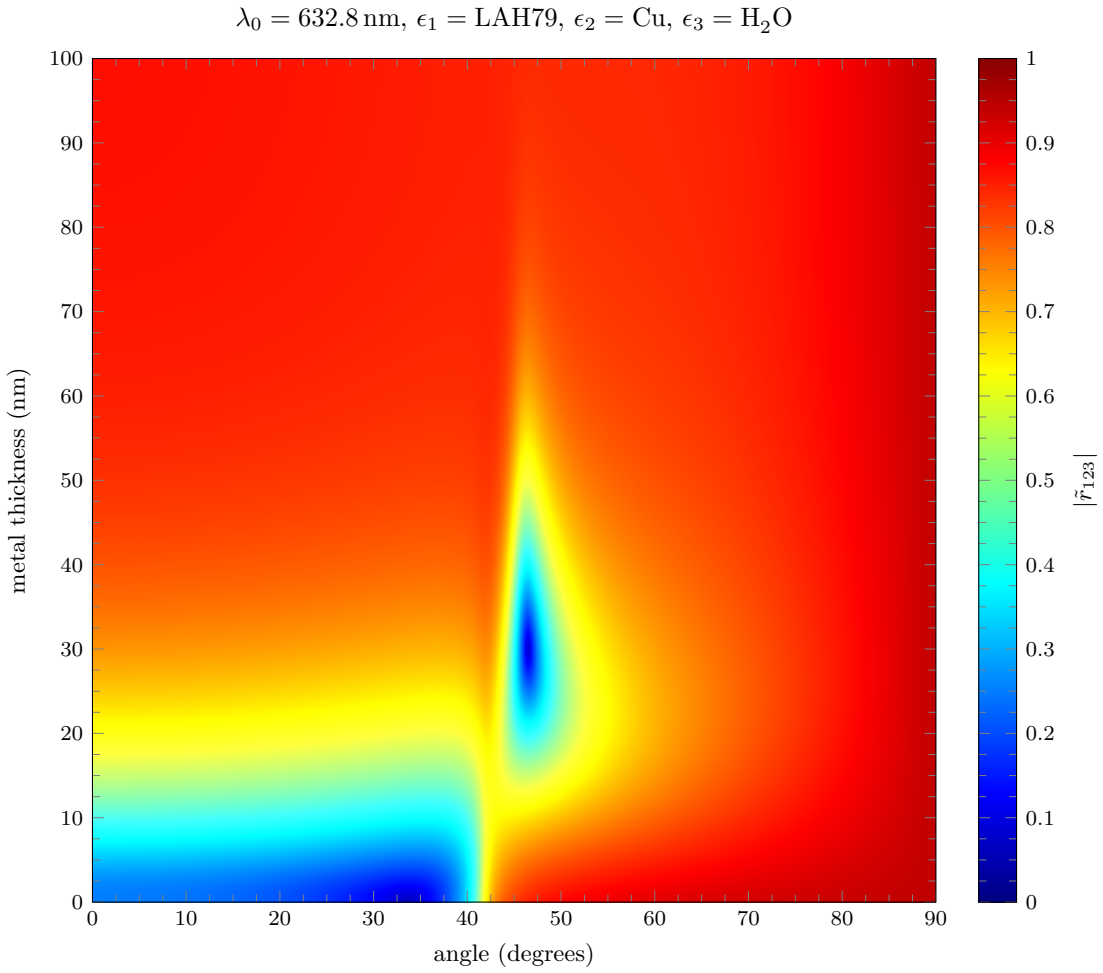

Figure 39: Reflection coefficent $|\tilde{r}_{123}|$ for the three layer fresnel system (Cu-LAH79-H_2O) as a function of incident angle and thickness of the metal layer ϵ_2. Numeric values of the permittivity are found in Table **??**

0.4.7 Ni-LAH79-H_2O

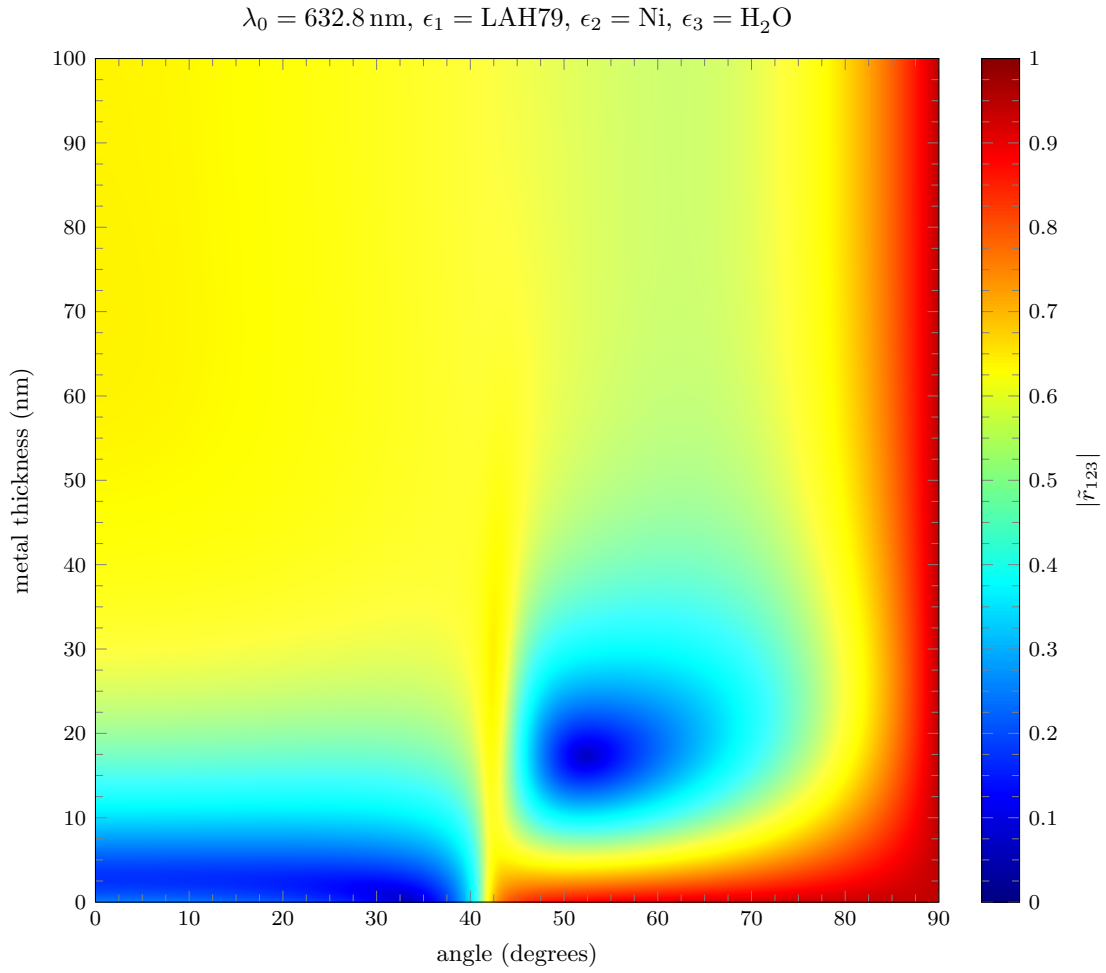

Figure 40: Reflection coefficent $|\tilde{r}_{123}|$ for the three layer fresnel system (Ni-LAH79-H_2O) as a function of incident angle and thickness of the metal layer ϵ_2. Numeric values of the permittivity are found in Table **??**

0.4.8 Pd-LAH79-H_2O

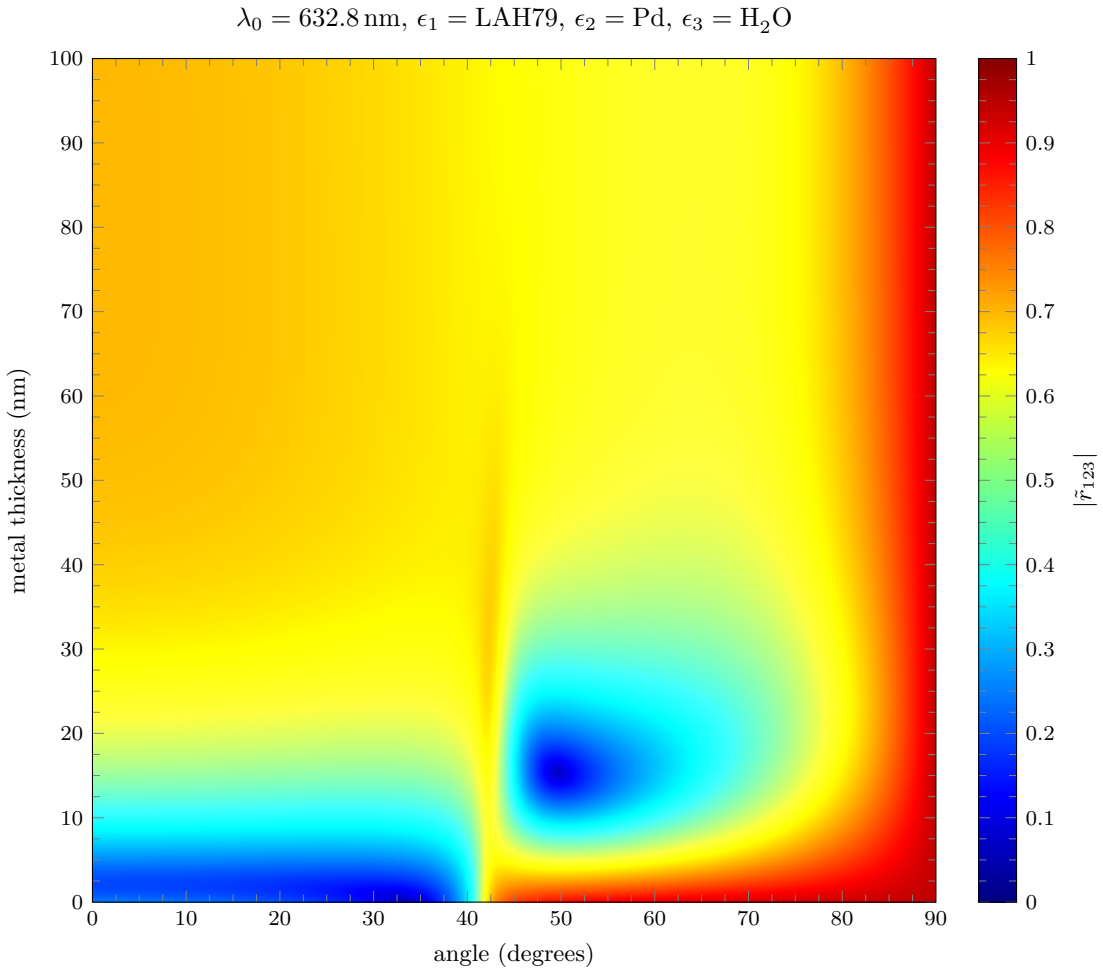

Figure 41: Reflection coefficent $|\tilde{r}_{123}|$ for the three layer fresnel system (Pd-LAH79-H_2O) as a function of incident angle and thickness of the metal layer ϵ_2. Numeric values of the permittivity are found in Table **??**

0.4.9 Pt-LAH79-H_2O

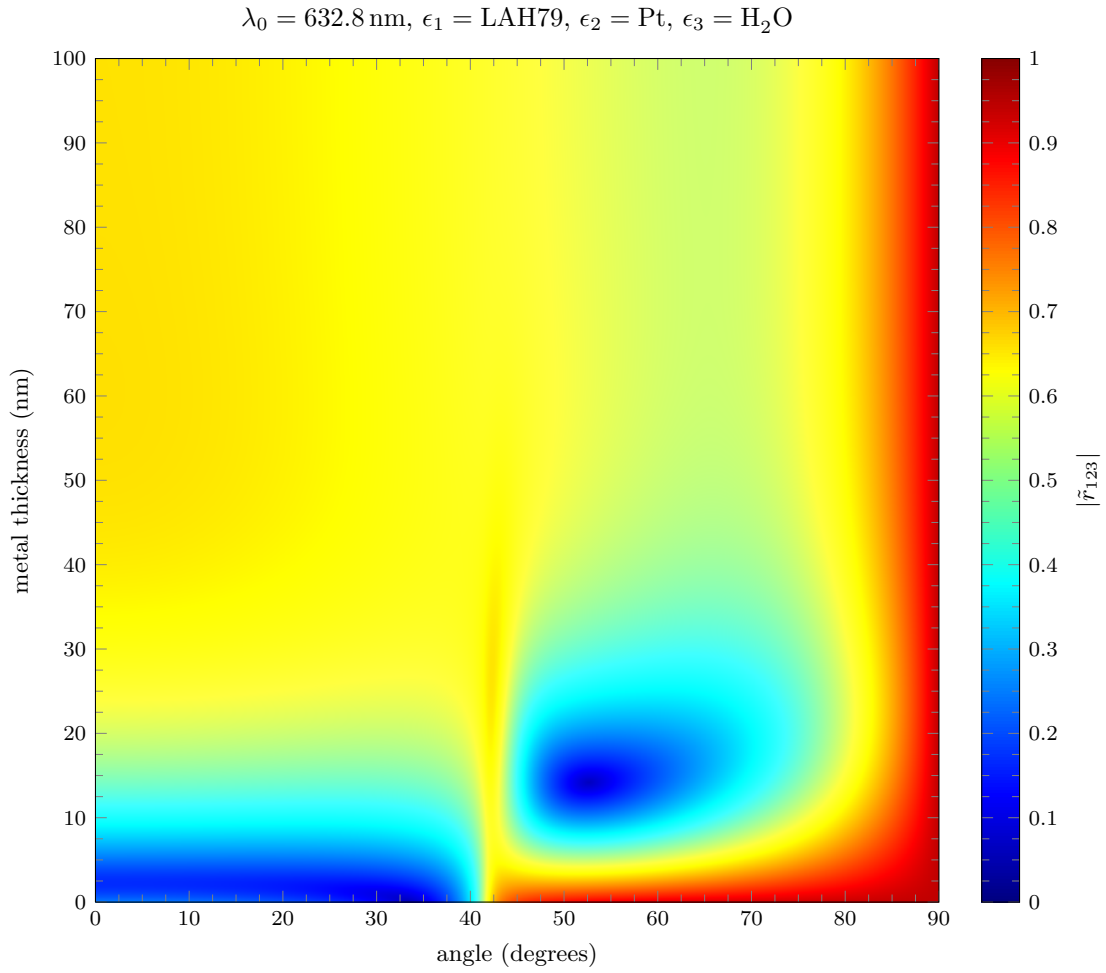

Figure 42: Reflection coefficent $|\tilde{r}_{123}|$ for the three layer fresnel system (Pt-LAH79-H_2O) as a function of incident angle and thickness of the metal layer ϵ_2. Numeric values of the permittivity are found in Table **??**

0.4.10 Ti-LAH79-H_2O

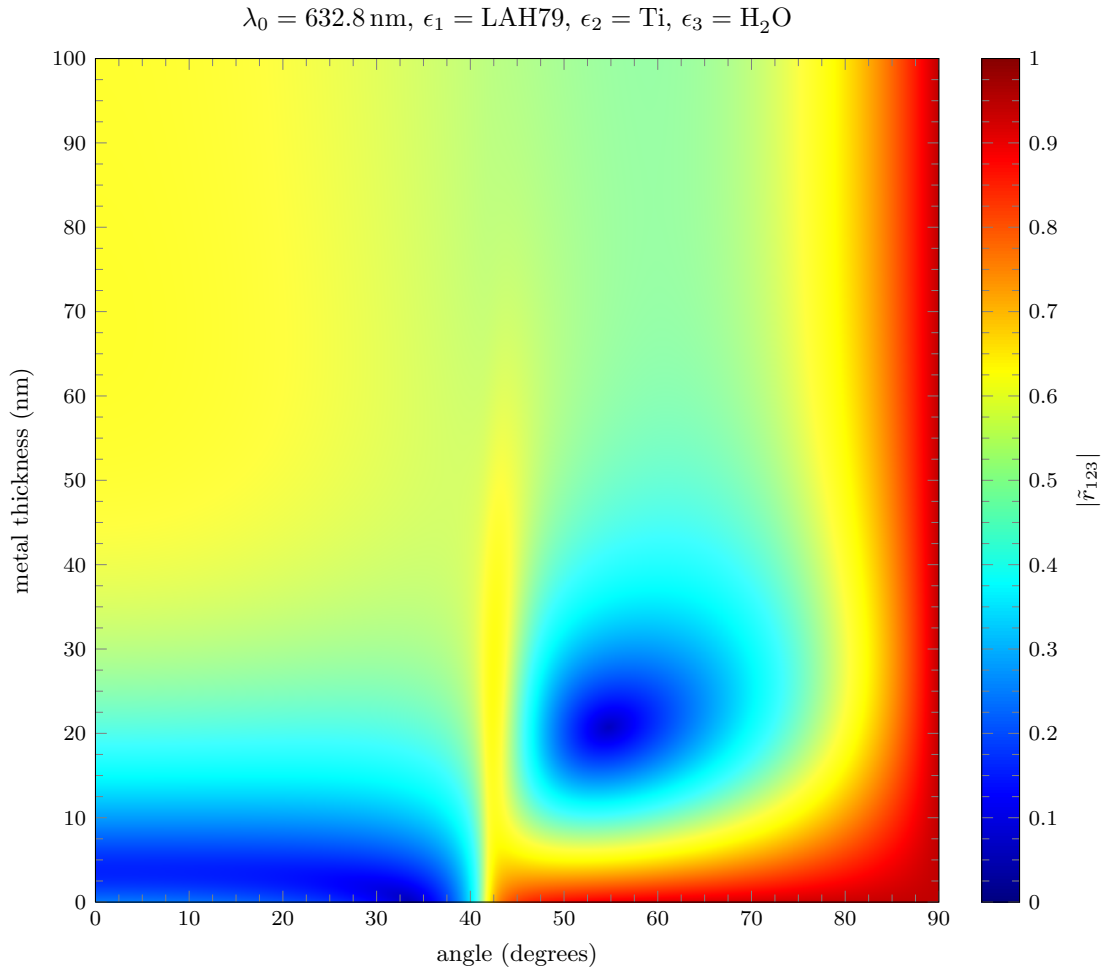

Figure 43: Reflection coefficent $|\tilde{r}_{123}|$ for the three layer fresnel system (Ti-LAH79-H_2O) as a function of incident angle and thickness of the metal layer ϵ_2. Numeric values of the permittivity are found in Table **??**

0.4.11 W-LAH79-H_2O

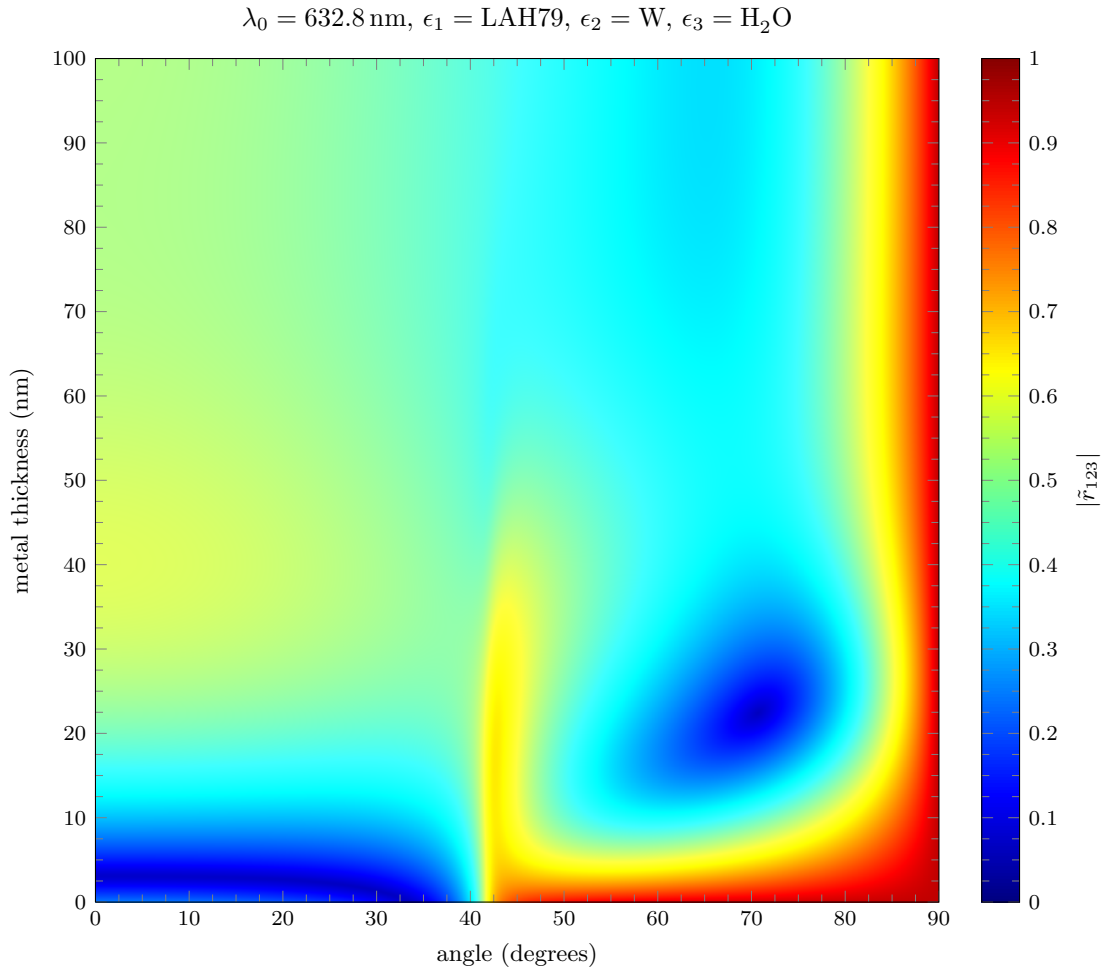

Figure 44: Reflection coefficent $|\tilde{r}_{123}|$ for the three layer fresnel system (W-LAH79-H_2O) as a function of incident angle and thickness of the metal layer ϵ_2. Numeric values of the permittivity are found in Table **??**